This is a repository copy of *Modelling of Chemical Process Plant*.

White Rose Research Online URL for this paper:
http://eprints.whiterose.ac.uk/75889/

Monograph:

Edwards, J.B. (1979) Modelling of Chemical Process Plant. Research Report. ACSE Report 96 . Department of Control Engineering, University of Sheffield, Mappin Street, Sheffield. Report also published in textbook " Modelling of Dynamical Systems" 1980

MODELLING OF CHEMICAL PROCESS PLANT

BY

J.B. Edwards, B.Sc.(Eng.), M.Sc., C.Eng., M.I.E.E., A.M.E.M.E.

Senior Lecturer in the Department of Control Engineering,
University of Sheffield,
Mappin Street,
Sheffield S13JD.

Research Report No. 96

July 1979

CHAPTER 2

Modelling of Chemical Process Plant

2.1 Introduction

A chemical plant involves the following basic operations, or stages:

(a) raw-material handling and preparation

(b) the chemical reaction itself

and (c) the separation of the various saleable products from one another and from the waste products.

In practice, however, the three operations may not take place separately. The rate of a chemical reaction, for instance, may be determined not so much by chemical kinetics as by the mechanical process of mixing the reagents (the reacting components) within the reactor if these are not freely miscible. Fluid and solid mechanics may therefore dominate even the chemical reaction stage (b) of production in some instances. In other situations, thermodynamics may play the dominant role in the reactor since the velocity of chemical reaction is often highly temperature-dependent and furthermore, large quantities of heat can be generated or absorbed in the course of the reaction. Thermal considerations are obviously of paramount importance in such cases. Conversely, the separation stage (c), although frequently involving the thermodynamic process of distillation or perhaps the fluid mechanical process of solvent extraction may nevertheless be affected by the continuing reaction of unused reagents within the separation vessel after these have left the reactor proper.

As a final example of the difficulty of categorising real life operations we should also note that even the preparation stage (a) may also involve more than just the grading and premixing of reagents: as in the case of preparing sinter feeds for the blast furnace where mechanical

transportation and combustion take place simultaneously.

The isolation of three sequential stages in chemical production is therefore only an idealising concept. Likewise the basic physical and chemical phenomena (or processes) involved, viz.

(i) mass transfer

(ii) heat transfer

and (iii) chemical change

do not take place completely separately and cannot in general be associated uniquely with any of the three production stages (a), (b) or (c). It is nevertheless essential to study idealised systems dominated by single isolated processes to acquire insight into their behaviour before proceeding to large scale simulation or pilot plant studies of systems involving all three phenomena operating in parallel because of the risk of error (from human, numerical or instrumentation sources) and the often unmanageable number of degrees of freedom otherwise presented by full-scale process simulation.

This chapter therefore sets out to show how idealised unit processes might be modelled analytically so that expected approximate solutions may be generated against which full-scale system simulations can be tested.

2.2 Setting up the process equations

Process equations are formulated from fairly elementary concepts of physical and chemical dynamic balance and equilibrium. Three system examples are considered here each dominated by a different process from the list (i), (ii), (iii) (above). We consider first an elementary, liquid/liquid head exchanger of the counterflow type.

2.2.1 Heat-exchanger example

The system is illustrated diagramatically in Fig. 2.1. The two liquids flow in opposite directions parallel to one another at mass rates W_1 and W_2 and separated by a heat-conducting interface which will be assumed to have

negligible thermal capacitance or resistance. The outer shell is assumed to be perfectly insulating. For modelling purposes the process is first imagined to be subdivided into N cells each of length $\delta h'$ and all identical except that cells 1 and N have atypical conditions pertaining at their left-and right-hand boundaries respectively. (These are the process boundary conditions to be discussed later). Within each cell conditions are assumed to be completely homogeneous either side the interface so that the temperatures of the two fluids 1 and 2 within cell n may be represented by the single variables $\theta_1(n,t)$ and $\theta_2(n,t)$ respectively. The functions $\theta_1(h',t)$ and $\theta_2(h',t)$, where h' denotes a general distance from the left-hand process boundary, are therefore approximated initially by spatially discrete-functions $\theta_1(n,t)$ and $\theta_2(n,t)$, n = 1,2 ...N, which undergo step-changes at each cell boundary. This is an example of the use of the "stirred-tank concept" employed in process modelling : each cell being thought of as a discrete tank the contents of which are thoroughly mixed.

There being no chemical change in this process, it is now necessary merely to draw up an inventory of the material and heat entering and leaving each cell (or tank) compartment, any imbalance between inflow and outflow being equated to a rate of build-up of material or heat within the compartment. The material balance is trivial in this example (if the fluids are assumed to be incompressible, of constant density and completely filling the cells at all times) yielding merely the result that W_1 and W_2 are functions of time only and invariant in h'. The heat balance for the system is more complicated however and, for fluids 1 and 2 in cell n, may be written

$$\left.\begin{array}{l} S_1\ \rho_1\ A_1\ \delta h'\ d\ \theta_1(n,t)/dt = W_1 S_1\ \{\theta_1(n-1,t) - \theta_1(n,t)\} + \delta q(n,t) \\ S_2\ \rho_2\ A_2\ \delta h'\ d\ \theta_2(n,t)/dt = W_2 S_2\ \{\theta_2(n+1,t) - \theta_2(n,t)\} - \delta q(n,t) \end{array}\right\} \quad (2.1)$$

where the suffixes apply to the associated fluids and compartments, S

denotes specific heat, ρ fluid density and A the cross-sectional area of
the flow passage. $\delta q(n,t)$ is the rate of heat flow across the interface
from liquid 2 to liquid 1 and is proportionally dependent upon the temperature difference between the liquids and the interface wall and also
upon the interface area $\pi\, d\delta h'$ (where d is the interface tube diameter).
The major resistance to heat flow is provided by thin boundary layers of
near-stationary liquid, lining both sides of the interface, the thicknesses
of which are found to decrease with flow-rate. In fact it is found that
this resistance is proportional to $W^{-0.8}$ so that:

$$\delta q(n,t) = k_1 \ \pi \ d \ W_1^{0.8}\{\theta_i(n,t) - \theta_1(n,t)\} \ \delta h'$$

$$= k_2 \ \pi \ d \ W_2^{0.8} \ \{\theta_2(n,t) - \theta_i(n,t)\} \ \delta h'$$

where k_1 and k_2 are constant coefficients of heat transfer. θ_i denotes
interface temperature, and may be eliminated from the two equations above
to give

$$\delta q(n,t) = \frac{k_1 \ k_2 \ \pi \ d \ (W_1 W_2)^{0.8}\{\theta_2(n,t) - \theta_1(n,t)\}\delta h'}{k_1 W_1^{0.8} + k_2 W_2^{0.8}} \qquad (2.2)$$

Given the constant parameters of the system and input functions
$W_1(t)$, $W_2(t)$, $\theta_1(o,t)$ and $\theta_2(N,t)$ equation 2.1 and 2.2 are suitably
expressed for computer simulation of the system provided a value for N
can be specified for solutions of the desired accuracy. For analytical
solution however we require a much more compact model representation.

Now the true temperature functions will be continuous in time and space
between the boundaries (at $h' = 0$ and L' in this case) and will therefore
be governed by Taylor series so that

$$\theta_1(n,t) - \theta_1(n-1,t) = \frac{\partial\theta_1(n,t)}{\partial h'} \ \delta h' - \frac{1}{2}\frac{\partial^2\theta_1(n,t)(\delta h')^2}{(\partial h')^2} + \text{higher powers of } \delta h'$$

and

$$\theta_2(n+1,t) - \theta_2(n,t) = \frac{\partial\theta_2(n,t)}{\partial h'} \ \delta h' + \frac{1}{2}\frac{\partial^2\theta_2(n,t)(\delta h')^2}{(\partial h')^2} + \text{higher powers of } \delta h'$$

$$(2.3)$$

and as $\delta h'$ is made progressively smaller for a given length L' of process, i.e. as N, $(= L'/\delta h')$ is made progressively larger, the approximate discrete temperature functions governed by (2.1) and the continuous functions governed by (2.3) will tend to equality so that we are justified in substituting (2.3) in (2.1) if $\delta h' \to 0$, yielding:

$$S_1 \rho_1 A_1 \frac{\partial \theta_1}{\partial t} = - W_1 S_1 \frac{\partial \theta_1}{\partial h'} + \frac{k_1 k_2 \pi d (W_1 W_2)^{0.8} (\theta_2 - \theta_1)}{k_1 W_1^{0.8} + k_2 W_2^{0.8}}$$

and

$$S_2 \rho_2 A_2 \frac{\partial \theta_2}{\partial t} = W_2 S_2 \frac{\partial \theta_2}{\partial h'} - \frac{k_1 k_2 \pi d (W_1 W_2)^{0.8}}{k_1 W_1^{0.8} + k_2 W_2^{0.8}} (\theta_2 - \theta_1)$$

$$, \quad 0 < h' < L' \quad (2.4)$$

Later in the chapter we shall consider further a symmetrically built and operated process, i.e. one in which $A_1 = A_2 = A$, $k_1 = k_2 = k$, $S_1 = S_2 = S$, $\rho_1 = \rho_2 = \rho$, operated under the nominal working condition

$$W_1 = W_2 = W \tag{2.5}$$

under which circumstances (2.4) simplifies to the normalised form

$$\partial \theta_1 / \partial \tau = -\partial \theta_1 / \partial h + \theta_2 - \theta_1$$
$$\partial \theta_2 / \partial \tau = \partial \theta_2 / \partial h - \theta_2 + \theta_1 \tag{2.6.}$$

where τ and h denote normalised time and distance, given by

$$\tau = t/T_n$$
$$h = h'/L_n \tag{2.7}$$

where

$$T_n = 2 S \rho A/(k \pi d W^{0.8})$$
$$L_n = 2 S W^{0.2}/(k \pi d) \tag{2.8}$$

It is interesting to note that base time T_n is the time for either fluid to travel base distance L_n that in turn has an important physical significance which will become apparent later.

2.2.2 Binary distillation column

(a) Packed type

Distillation columns too are counterflow processes like the heat exchanger discussed above and can exhibit similarities in their behavioural characteristics. There are, however, important differences in their comparative behaviour resulting largely from the very different boundary conditions which apply in the two cases. These will be examined later but for the moment we shall concentrate on the development of the system's partial differential equations (p.d.e's) which will be found to closely resemble those of the heat exchanger. The system is illustrated by Figs. 2.2, which shows the two-stage constructuion of columns, involving two sections: the rectifier and the stripping section, and 2.3 which illustrates a conceptual cell of the rectifier, again assumed to be thoroughly mixed. Vapour and liquid streams flow past one another as shown at rates denoted by V and L moles* p.u. time, the streams being composed of mixtures of the two components to be separated by the column. X denotes the mole*-fraction (composition) óf the more-volatile- (lighter-) component in the liquid mixture and Y that in the vapour stream. Primes are associated with the variables in the stripping section and suffixes s and r associated with the flow-rates denote stripping-section and rectifier quantities respectively. As Fig. 2.2 shows, boiling mixture is fed into the column between stages, the liquid entering at flow rate F_ℓ, composition Z and the vapour at flow rate F_v, composition z. Products are withdrawn from the process at top and bottom, i.e. from the accumulator and reboiler at rates $V_r - L_r$ and $L_s - V_s$ and at composition $X(N + 1)$, $Y'(-M-1)$ respectively. The object of the distillation

---

* One mole of an element or compound has a weight numerically equal to the molecular weight expressed in the chosen system of units, e.g., one mole of water in S.I. units weighs $2 + 16 = 18$ kg.

is to make X(N+1) as close to unity as possible and Y'(-M-1) close to zero
at as high a throughput as possible and with a minimum energy utilisation
i.e. with minimum recirculation flow. (Economic factors clearly determine
the optimum compromise between these conflicting requirements).

Column sections of the "packed type" are deliberately filled with
solid, pourous packing material to produce a spatial distribution of com-
position through the column so again necessitating consideration of an
infinitessimal cell illustrated in Fig. 2.3. Within each cell evaporation
and condensation occur and under adiabatic conditions, if the two compo-
nents have equal molecular latent heats, each mole condensing, of whatever
component, causes another to evaporate. If only latent heats are consi-
dered therefore, (sensible heat changes being assumed negligible by
comparison), the heat-balance for each cell is trivial and merely constrains
the flow rates, V_r, V_s, L_r and L_s to be spatially invariant, (as in the
heat exchanger considered earlier but for different reasons).

In this process, unlike the heat-exchanger, it is the material-balance
which produces the significant dynamic effects. If H_{rv}, $H_{r\ell}$, H_{sv} and $H_{s\ell}$
denote the fixed molar capacitance p.u. length of the rectifier and stripping
section for vapour and liquid respectively, then material-balances for the
lighter component taken on elementary slices of the two sections produce
the following differential equations

$$\left.\begin{array}{l} H_{rv} \dfrac{dY}{dt}(n,t)\, \delta h' = V_r \{Y(n-1,t) - Y(n,t)\} + k_r \{Y_e(n,t) - Y(n,t)\}\delta h' \\[3mm] H_{r\ell} \dfrac{dX(n,t)}{dt}\delta h' = L_r\{X(n+1,t) - X(n,t)\} - k_r\{Y_e(n,t) - Y(n,t)\}\delta h' \end{array}\right\} \begin{array}{l} n > 1 \\[3mm] (2.9) \end{array}$$

$$\left.\begin{array}{l} H_{sv} \dfrac{dY'(n,t)}{dt}\delta h' = V_s\{Y'(n-1,t) - Y'(n,t)\} + k_s\{X'(n,t) - X'_e(n,t)\}\delta h' \\[3mm] \text{and} \\[3mm] H_{s\ell} \dfrac{dX'(n,t)}{dt}\delta h' = L_s\{X'(n+1,t) - X'(n,t)\} - k_s\{X'(n,t) - X'_e(n,t)\}\delta h' \end{array}\right\} \begin{array}{l} n< -\,1 \end{array}$$

$$(2.10)$$

where k_r and k_s are constant coefficients of evaporation and suffix 'e' indicates _equilibrium_ quantities. The terms involving these quantities (above) represent the net rate of evaporation of the lighter component i.e. the cross-flow from the liquid to the vapour phase which ceases in situations where neighbouring liquid and vapour mixtures are in so-called "thermodynamic equilibrium" with one another. For ideal mixtures, (those obeying Dalton's and Rayoult's Laws), the equilibrium relationship may be shown[1] to be

$$\beta = Y_e (1 - X)/ \{X(1 - Y_e)\} \qquad (2.11)$$

where Y_e is the composition of a vapour in equilibrium with a liquid of composition X, and, in terms of stripping section quantities:

$$\beta = Y'(1 - X_e')/ \{X_e'(1 - Y')\} \qquad (2.12)$$

where X_e' is the composition of a liquid mixture with which vapour of composition Y' would produce equilibrium. The parameter β is nearly constant for a given ideal mixture and is termed the "relative volatility" of the mixture.

A typical equilibrium curve is sketched in Fig. 2.4 from which the symmetry about the $- 45^o$ line should be noted. β is greater than unity but the smaller its value the closer the curve approaches the $+ 45^o$ line (i.e. the smaller the difference between the vapour and liquid compositions of equilibrium mixtures and the more difficult the distillation). For convenience of subsequent dynamic analysis, the curve is usually approximated[2] by two linear relationships, (one for the rectifier and the other for the stripping section), these being

$$\alpha(1 - Y_e) = 1 - X \qquad (2.13)$$

and $\qquad \alpha X_e' = Y' \qquad (2.14)$

where the straight-line slopes are constrained thus;

$$\beta > \alpha > 1 \qquad (2.15)$$

so that, eliminating X and Y' using (2.13) and (2.14), we obtain

$$H_{rv} \frac{dY(n,t)\delta h'}{dt} = V_r\{Y(n-1,t) - Y(n,t)\} + k_r\{Y_e(n,t) - Y(n,t)\}\delta h' \left.\vphantom{\frac{dY}{dt}}\right\}$$

$$\alpha H_{r\ell} \frac{dY_e(n,t)\delta h'}{dt} = \alpha L_r\{Y_e(n+1,t) - Y_e(n,t)\} - k_r\{Y_e(n,t) - Y(n,t)\}\delta h' \left.\vphantom{\frac{dY}{dt}}\right\}$$

$$n > 1$$

$$(2.16)$$

and

$$H_{s\ell} \frac{dX'(n,t)\delta h'}{dt} = L_s\{X'(n+1,t) - X'(n,t)\} - k_s\{X'(n,t) - X_e'(n,t)\} \left.\vphantom{\frac{dX}{dt}}\right\}$$

$$\alpha H_{sv} \frac{dX_e' \, \delta h'}{dt} = \alpha V_s \{X_e'(n-1,t) - X_e'(n,t)\} + k_s\{X'(n,t) - X_e'(n,t)\} \left.\vphantom{\frac{dX}{dt}}\right\}$$

$$n < -1$$

$$(2.17)$$

We therefore have situations pertaining in the two column sections very similar in mathematical structure to those applying within the heat-exchanger (c.f. equations (2.1) and (2.2)) so that applying Taylor's theorem and letting $\delta h' \to 0$, as before, yields the p.d.e's

$$H_{rv} \, \partial Y/\partial t = -V_r \, \partial Y/\partial h' + k_r(Y_e - Y) \left.\vphantom{\frac{Y}{t}}\right\}$$

$$\alpha H_{r\ell} \, \partial Y_e/\partial t = \alpha L_r \, \partial Y_e/\partial h' - k_r(Y_e - Y) \left.\vphantom{\frac{Y}{t}}\right\}$$

$$h' > 0 \qquad (2.18)$$

$$H_{s\ell} \, \partial X'/\partial t = L_s \, \partial X'/\partial h' + k_s(X_e' - X') \left.\vphantom{\frac{X}{t}}\right\}$$

$$\alpha H_{sv} \, \partial X_e'/\partial t = -\alpha V_s \, \partial X_e'/\partial h' - k_s(X_e' - X') \left.\vphantom{\frac{X}{t}}\right\}$$

$$h' < 0 \qquad (2.19)$$

again very similar to those for the heat-exchanger.

If we again confine attention to a symmetrical plant, i.e. one in which

$$\alpha H_{r\ell} = H_{s\ell} = H \left.\vphantom{\frac{H}{H}}\right\}$$

$$H_{rv} = \alpha H_{sv} = c H \left.\vphantom{\frac{H}{H}}\right\}$$

$$k_r = k_s = k \left.\vphantom{\frac{H}{H}}\right\}$$

$$(2.20)$$

where c is a constant, and operated under the nominal working conditions

$$V_r = \alpha L_r = L_s = \alpha V_s = V \qquad (2.21)$$

then normalising the p.d.e's (2.18) and (2.19) yields the simplified system:

$$c \, \partial Y/\partial \tau = -\partial Y/\partial h + Y_e - Y \left.\vphantom{\frac{Y}{\tau}}\right\}$$

$$\partial Y_e/\partial \tau = \partial Y_e/\partial h - Y_e + Y \left.\vphantom{\frac{Y}{\tau}}\right\}$$

$$, \quad h > 0 \qquad (2.22)$$

$$\left.\begin{array}{l} \partial X'/\partial \tau = \partial X'/\partial h + X'_e - X' \\ c\partial X'_e/\partial \tau = -\partial X'_e/\partial h - X'_e + X' \end{array}\right\} \quad , \quad h < 0 \qquad (2.23)$$

where τ and h denote <u>normalised</u> time and distance, being given by

$$\tau = t/T_n \qquad (2.24)$$

$$h = h'/L_n \qquad (2.25)$$

where $T_n = H/k$ $\qquad (2.26)$

and $\quad L_n = V/k$ $\qquad (2.27)$

Again the base distance/time ratio (L_n/T_n) = liquid velocity so that T_n is the time for the liquid to travel base distance L_n (the significance of which emerges later). The vapour/liquid capacitance ratio c will usually be $<< 1.0$ but in later analysis will be set at unity in the interests of ease of solution.

(b) Tray-type column

Industrial scale column sections are more usually physically segmented by the deliberate inclusion of barriers or "trays" holding constant volumes of liquid which cascades down the column from tray to tray. The vapour forces its way up through the trays by lifting so called "bubble-caps" which act as non-return valves. With this construction a discretely changing spatial distribution of composition is achieved and our hitherto <u>conceptual</u> cells now acquire a definite physical significance. With this type of column it is generally assumed that the liquid and vapour above any given tray are in continuous equilibrium with one another and vapour capacitance is either neglected or lumped with the liquid capacitance. H_{rv} and H_{sv} are therefore put to zero in (2.9) and (2.10) and k_r and k_s made infinite so that

$$Y_e(n,t) = Y(n,t) \quad , \quad n > 1$$

and $\qquad X'_e(n,t) = X(n,t) \quad , \quad n < 1 \qquad (2.28)$

yielding general tray equations

$$\alpha H_{r\ell} \frac{dY(n,t)}{dt} \delta h' = \alpha L_r \{Y(n+1) - Y(n,t)\} + V_r \{Y(n-1,t) - Y(n,t)\} \qquad n > 1$$

and

$$H_{s\ell} \frac{dX'(n,t)}{dt} \delta h' = L_s \{X'(n+1) - X'(n,t)\} + \alpha V_s \{X'(n-1,t) - X'(n,t)\} \quad n < -1$$

(2.29)

$\delta h'$ here, of course, denotes the actual finite length of column between trays. Together with the boundary conditions, yet to be considered, numerical solution may therefore be undertaken at this stage with the advantage over the heat-exchanger and packed-column that the total number of cells (trays in this case) is prespecified. For analytical solution however a p.d.e. representation is again preferable and is a permissible approximation when the column comprises a large number of trays: as is normally the case with industrial scale systems separating difficult mixtures. It is assumed that the discrete composition profiles may be closely approximated by spatially continuous functions so again permitting the use of the Taylor series to eliminate dependent variables other than $Y(n,t)$ and $X'(n,t)$, giving

$$\alpha H_{r\ell} \frac{\partial Y}{\partial t} = (\alpha L_r - V_r) \frac{\partial Y}{\partial h'} + \frac{(\alpha L_r + V_r)}{2} \frac{\partial^2 Y}{(\partial h')^2} \delta h' \quad , \quad h' > 0$$

and

(2.30)

$$H_{s\ell} \frac{\partial X'}{\partial t} = (L_s - \alpha V_s) \frac{\partial X'}{\partial h'} + \frac{(L_s + \alpha V_s)}{2} \frac{\partial^2 X'}{(\partial h')^2} \delta h' \quad , \quad h' < 0$$

ignoring higher powers of $\delta h'$.

Under the symmetrical operating conditions (2.20) and (2.21), the system therefore reduces to the normalised form

$$\partial Y/\partial \tau = \partial^2 Y (\partial h)^2 \qquad , \qquad h > 0$$
$$\partial X'/\partial \tau = \partial^2 X'/(\partial h)^2 \qquad , \qquad h < 0$$

(2.31)

where again $\tau = t/T_n$ and $h = h'/L_n$

but the base time and distance are now given by

$$T_n = H \delta h'/V$$

and

$$L_n = \delta h'$$

(2.32)

The fundamental differences between the p.d.e's for packed-and tray-columns give rise to important differences in the dynamic behaviour as will be demonstrated later.

It should be emphasised that our treatment of columns has been confined to a consideration of composition dynamics. Columns are of course subject also to variations in internal pressure and in the levels of the end vessels, all of which interact with and are affected by the composition variations. The foregoing analysis has however, assumed that these variables can be closely regulated, which is generally the case but for a thorough investigation of these faster dynamics the reader is referred to the text of Rademaker et al[3]. Judson King[1] provides an excellent detailed coverage of steady-state column design.

2.2.3 The Tubular Chemical Reactor

Having demonstrated similarities (and differences) between the mathematical structure of ideal heat-, mass-transfer processes, we now examine the influence of chemical-change on process dynamics in situations where chemical kinetics dominate other factors. Mass-transfer will be seen to play an important role easily embraced by the analysis. Thermal effects, through often crucial, are more difficult to include and temperatures will therefore be regarded as perfectly regulated in our investigation of the "tubular" (spatially-distributed) reactor. Uncontrolled temperature variations will, however, be examined afterwards in a consideration of the continuous stirred-tank reactor described by a lumped parameter model.

We consider the simple liquid reaction in which reagents A and B react together to form the single product C. For generality we will initially consider the reaction to be of the reversible type permitting C to decompose back into A and B. The stoichiometric equation for the reaction is therefore

$$A + B \rightleftharpoons 2C \tag{2.33}$$

indicating that one mole of A reacts with one mole of B to form two moles of C and vice versa. (In practice the situation can be much more complicated involving gaseous and solid materials, intermediate products, several reactions taking place sequentially and in parallel, and the

influence of catalysts etc., but the overall mechanism can often be constructed from a conceptual network of elementary systems of the sort examined . here).

Because of equation (2.33) we must now account for a new phenomenon in our basic concepts of dynamic balance: that of one type of material (mixture A and B in this case) changing into another type (here, product C). We therefore become involved with rates of chemical reaction which are found[4] from the kinetic theory of gasses, and experimentally, to be governed by equations of the type

$$r_c = k_1 [A]^\alpha [B]^\beta \qquad (2.34)$$

and
$$r_{ab} = k_2 [C]^\gamma \qquad (2.35)$$

where r_c denotes the rate of generation of C (and r_{ab} that of A and B) expressed in molés p.u. volume of mixture p.u. time, and the square brackets indicate <u>concentrations</u> of the appropriate substance expressed in moles per unit volume of the overall mixture. The <u>velocity coefficients</u> k_1 and k_2 are, for ideal gasses, functions only of absolute temperature θ taking the form

$$k_1 = a_1 \exp(- \theta_{b1}/\theta) , \quad k_2 = a_2 \exp(-\theta_{b2}/\theta) \qquad (2.36)$$

(where a_1, θ_{b1}, a_2 and θ_{b2} are constants) and are frequently assumed to be nearly so for reactions involving liquids and other none-ideal materials. The indices α, β and γ in (2.34) and (2.35) are usually small integers (or their reciprocals) generally determined experimentally.

Considering now the tubular reactor, a short section of which is illustrated in Fig. 2.5, then for conceptual cell n of length $\delta h'$ and volume δV we may write down a material balance for any one of the three component substances A B or C, taking account of the fact that components can now change from one to another, within the cell considered, at rates governed by equations of the type (2.34) and (2.35). Choosing C, the material balance for this substance may be written

$$\delta V \frac{d[C(n,t)]}{dt} = F\{[C(n-1,t)] - [C(n,t)]\} + \delta V\{k_1 [A(n,t)]^\alpha [B(n,t)]^\beta$$
$$- k_2 [C(n,t)]^\gamma\} \qquad (2.37)$$

where F is the volumetric flow-rate of mixture through the reactor.

Now if one mole of A,B or C occupy identical volumes, i.e. if the substances are _ideal_, then the molar density ρ_m of the overall mixture will be unchanged throughout, i.e.

$$\rho_m , = [A(n,t)] + [B(n,t)] + [C(n,t)] = \text{a constant} \qquad (2.38)$$

and if reagents are fed in stoichiometric proportions (equal portions in this example) then

$$[A(n,t)] = [B(n,t)] \qquad (2.39)$$

so that

$$[A(n,t)] = [B(n,t)] = 0.5\{\rho_m - [C(n,t)]\} \qquad (2.40)$$

permitting (2.37) to be expressed in terms of C only. The resulting differential equation becomes

$$\delta V \frac{d[C(n,t)]}{dt} = F\{[C(n-1,t)] - [C(n,t)]\}$$
$$+ \delta V \{k_1 \rho_m /2 - (k_1/2 + k_2)[C(n,t)]\} \qquad (2.41)$$

if the reaction is of _first-order_ with respect to $[C]$, i.e. if

$$2 \alpha = 2 \beta = \gamma = 1.0 \qquad (2.42)$$

Alternatively, the composition of C could be expressed in terms of its mole-fraction, X, rather than $[C]$, the number of moles p.u. volume, since

$$\rho_m X = [C] \qquad (2.43)$$

equation (2.41) thus becoming

$$\delta V \frac{dX(n,t)}{dt} = F\{X(n-1,t) - X(n,t)\} + \delta V\{k_1/2 - (k_1/2+k_2)X(n,t)\}$$
$$(2.44)$$

from which we deduce, in a manner similar to that used for the previous examples, the p.d.e

$$\partial X/\partial t = -(F/a)\partial X/\partial h' + (k_1/2 + k_2)\{k_1/(k_1 + 2k_2) - X\} \qquad (2.45)$$

where, a, is the cross-sectional area of the reactor tube.

Now $k_1/(k_1 + 2k_2)$ is the equilibrium value, X_e, which X would acquire were the reaction to take place in a <u>closed system</u>, such as a batch reactor, for a sufficient length of time. Under such circumstances backward and forward rates of reaction r_c and r_{ab} ultimately balance so that if suffix e denotes <u>equilibrium values</u>, then from (2.34) and (2.35) we get

$$k_2 \left[C_e\right]^\gamma = k_1 \left[A_e\right]^\alpha \left[B_e\right]^\beta \tag{2.46}$$

which in our case reduces to

$$k_2 \left[C_e\right] = k_1 \left[A_e\right]^{0.5} \left[B_e\right]^{0.5} = k_1 \left[A_e\right] \tag{2.47}$$

if the initial charge of reagents were in stoichiometric proportion. Since, in general,

$$\left[A\right] + \left[B\right] + \left[C\right] = \rho_m \tag{2.48}$$

and, in our case $\left[A\right] = \left[B\right]$, then

$$2\left[A\right] = \rho_m - \left[C\right] \tag{2.49}$$

so that, substituting for $\left[A_e\right]$ in (2.47) we get

$$\left[C_e\right] = k_1 \rho_m/(k_1 + 2k_2)$$

or

$$X_e = k_1/(k_1 + 2k_2) \tag{2.50}$$

and so (2.45) becomes

$$\partial X/\partial t = - U \, \partial X/\partial h' + (k_1/2 + k_2)(X_e - X) \tag{2.51}$$

where U is the fluid velocity. The equation may again be normalised giving a result identical but for the symbols to the previous spatially continuous examples, viz.

$$\partial X/\partial \tau = - \partial X/\partial h + X_e - X \tag{2.52}$$

where $\tau = t/T_n$ and $h = h'/L_n$ and in this case

$$\left. \begin{aligned} T_n &= (k_1/2 + k_2)^{-1} \\ L_n &= U(k_1/2 + k_2)^{-1} \end{aligned} \right\} \tag{2.53}$$

and

2.3 Similarities and differences in mathematical structure of the system models

In all three cases of the truly spatially-continuous processes examined, the p.d.e's have involved only the first-derivatives of the dependent variables with respect to space and time and cross-flow terms dependent upon the departure of these variables from their equilibrium

values, ($\theta_2(n,t)$ is the equilibrium value of $\theta_1(n,t)$ in the heat-exchanger example and vice versa). Indeed similar p.d.e's are widely encountered in chemical plant modelling generally. It would therefore appear that any approach capable of producing a solution to one example should also cope with others provided the boundary conditions involved in the latter are of no greater complexity. We shall therefore focus attention on the distillation column to illustrate an approach to model solution since the process clearly involves the most complex boundary conditions of the examples considered.

Before proceeding, however, it is important to notice an important difference between the first two examples and the chemical reactor arising in connection with the multiplicative nature of the process equations (2.1){and (2.2)}, (2.18), (2.19) and (2.51). In the first two examples simple products occur, each involving one dependent variable (or its derivative) and one independent variable (or some power thereof): the flow-rates in both cases being directly manipulable forcing functions. In the chemical reactor (equation 2.51), however, $k_1/2 + k_2$ is a dependent variable unless tight temperature control can be exercised throughout the reactor length. In view of the great sensitivity of k_1 and k_2 temperature θ (see equations 2.36) and the often considerable rate at which heat is released or absorbed by reaction, the control of temperature can unfortunately pose a problem of greater magnitude than that of controlling composition X itself. This problem is therefore examined briefly before proceeding to the solution of the p.d.e's. The following section will also serve incidentally to introduce the concept of linearisation in the fields of chemical process modelling.

2.4 Thermal characteristics of chemical reactors

The sometimes unusual nature of the thermal behaviour of reactors can be demonstrated by consideration of merely a single continuous stirred tank reactor (C.S.T.R) often employed in practice despite the less efficient

utilisation of the available volume compared to that achieved with a tubular reactor. The C.S.T.R. model is identical to that for a single cell representation of the tubular reactor and obtained by setting n = 1 in equation 2.41 and setting $[C(o,t)]$ to zero, assuming the reactor to be fed with reacgents only. We shall also assume an irreversible reaction in this analysis so that k_2 is also zero. Hence, dropping the spatial argument n (=1) of the variables we get

$$[\dot{C}(t)] = -(F/V) [C(t)] + \{k_1(\theta)/2\}\{\rho_m - [C(t)]\} \tag{2.54}$$

where the dot denotes the derivative with respect to time, t, V, the total reactor volume, is set equal to δV and argument θ is associated with velocity k_1 to emphasise its temperature dependence. In terms of X rather than $[C]$, therefore we obtain

$$\dot{X}(t) = - (F/V)X(t) + \{k_1(\theta)/2\} \{1 - X(t)\} \tag{2.55}$$

Now if θ is to vary, i.e.

$$\theta = \theta(t) \tag{2.56}$$

a heat balance is also necessary to complete the process model. We shall assume the reaction to be exothermic so that the rate of heat generation $q_g(t)$ by the reaction is given by

$$q_g(t) = \Delta H . r_c(t). V \tag{2.57}$$

where ΔH is the energy released per mole of C produced. $r_c(t)$ is the rate of generation of C in moles p.u. volume and given by equation (2.34) so that using equations (2.40), (2.42) and (2.43) we get

$$q_g(t) = \Delta H.V. \rho_m k_1(\theta) \{1 - X(t)\} \tag{2.58}$$

Now heat also enters the tank in the feed stream at a rate $F.H_c . \theta_a$ (if there is no preheating) and leaves in the outflow at a rate $F.H_c .\theta$, where θ_a is the ambient temperature and H_c the thermal capacitance p.u. volume of liquid. Heat will also be lost via the tank walls at a rate $Q_w(\theta-\theta_a)^*$

---

* Assuming Newton's law of cooling to hold.

where Q_w is constant and heat may be deliberately extracted by the immersion of, say, cooling tubes, at a rate $Q_t(\theta-\theta_c)$ where Q_t is an adjustable heat-transfer coefficient and θ_c the temperature of the cooling fluid, set for simplicity of analysis $= \theta_a$ in this example.* The heat-balance thus becomes

$$H_c V\dot{\theta}(t) = \Delta H. \, V\rho_m k_1(\theta) \, \{1-X(t)\} - (Q_t+Q_w + F \, H_c).\{\theta(t)-\theta_a\} \qquad (2.59)$$

and thus, together with (2.55) and (2.36) - which determines the variation of k_1 with θ, provides a complete description of the thermally uncontrolled reactor. The steady-state equations of the process, obtained by setting $\dot{X}$ and $\dot{\theta}$ to zero are

$$X = k_1(\theta)/\{k_1(\theta) + 2F/V\} \qquad (2.60)$$

and, eliminating $k_1(\theta)$ between the mass-and heat-balance equations,

$$X = \{(Q_t + Q_w)/F + H_c\}(\theta-\theta_a)/\Delta H. \, \rho_m \qquad (2.61)$$

the resulting curves of X versus θ being of sigmoid shape in the case of $(2.60)^\dagger$ and a straight-line in the case of (2.61) for constant Q_t and F. Depending upon the constant parameter values therefore, single or tripple points of intersection of the two curves are possible as illustrated in Fig. 2.6, suggesting the possibility of up to three steady-state working conditions.

2.4.1 Reactor Linearisation

The small-signal stability of the solutions may be investigated using the linearised, small-perturbation model of the system, derived by differentiating implicitly the nonlinear large-signal d.e's (2.55) and (2.59) and setting the differentials dX, $d\theta$, dF and dQ_t equal to small perturbations $x(t)$, $\phi(t)$, $f(t)$ and $q_t(t)$ respectively, giving

$$\begin{pmatrix} \dot{x} \\ \\ \dot{\phi} \end{pmatrix} = \begin{pmatrix} -(F/V+k_1/2) & , & 0.5(1-X)\partial k_1/\partial\theta \\ & & \Delta H. \, \rho_m(1-X)(\partial k_1/\partial\theta)/2H_c \\ - H.\rho_m k_1/2H_c & , & -(Q_t + Q_w + H_c F)/H_c V \end{pmatrix} \begin{pmatrix} x \\ \\ \phi \end{pmatrix} - \begin{pmatrix} X/V & , & 0 \\ \\ \dfrac{\theta-\theta_a}{V} & , & \dfrac{\theta-\theta_a}{H_c V} \end{pmatrix} \begin{pmatrix} f \\ \\ q_t \end{pmatrix} \qquad (2.62)$$

---

* θ_c will, of course, vary to some extent with θ but will be nearly constant if a large flow of coolant is used.

$\dagger$ Since k_1 increases monotonically with increasing θ (see equation 2.36)

Provided the perturbations are sufficiently small in magnitude compared to the steady-state values of the variables X, θ, F and Q_t, then solutions of the large-signal steady-state equations (2.60) and (2.61) may be substituted as quasi-constants in the coefficient matrices of (2.62) so yielding the desired linearised system.

If this system is written

$$
\begin{bmatrix} \dot{x} \\ \dot{\phi} \end{bmatrix} = \underline{A} \begin{bmatrix} x \\ \phi \end{bmatrix} + \underline{B} \begin{bmatrix} f \\ q_t \end{bmatrix} = \begin{bmatrix} a_{11}, & a_{12} \\ a_{21}, & a_{22} \end{bmatrix} \begin{bmatrix} x \\ \phi \end{bmatrix} + \begin{bmatrix} b_{11}, & b_{12} \\ b_{21}, & b_{22} \end{bmatrix} \begin{bmatrix} f \\ q_t \end{bmatrix} \tag{2.63}
$$

then the characteristic equation of the open-loop system is

$$
\text{Det} \begin{bmatrix} \underline{I}s - \underline{A} \end{bmatrix} = 0 \tag{2.64}
$$

giving, in this case,

$$
s = \{(a_{11} + a_{22}) \pm \sqrt{(a_{11} - a_{22})^2 + 4\, a_{12} a_{21}}\}/2 \tag{2.65}
$$

so that for open-loop stability, i.e. $R_e\, s < 0$,

$$
(a_{11} - a_{22})^2 + 4\, a_{12} a_{21} < (a_{11} + a_{22})^2
$$

and

$$
a_{11} + a_{22} < 0
$$

These conditions may be more simply expressed:

$$
a_{11}\, a_{22} > a_{12}\, a_{21} \tag{2.66}
$$

and

$$
a_{22} < -\, a_{11} \tag{2.67}
$$

and substituting for the elements of $\underline{A}$ in (2.66) using (2.62) readily yields the <u>necessary</u> stability condition that

$$
(1-X)\partial k_1/\partial\theta < 2(Q_t + Q_w + H_c F)(F/V + k_1/2)/F\Delta H.\rho_m \tag{2.68}
$$

whilst (2.67), after substitution, may be expressed

$$
(1-X)\partial k_1/\partial\theta < 2\{2H_c F(F/V) + H_c F k_1/2 + (Q_t + Q_w)(F/V)\}/F\Delta H.\rho_m \tag{2.69}
$$

It is interesting to note that (2.68) has the immediate graphical interpretation that the slope of the sigmoid curve (equation 2.60) in Fig. 2.6 should be less than that of the straight line (equation 2.61) and Denbigh[4] offers a physical interpretation of the condition regarding

the curves as heating and cooling characteristics respectively. The arguments are not mathematically rigorous however, (as he acknowledges) and the second condition (2.69) cannot be safely disregarded in general. The question is pursued more thoroughly by Himmelblau[5], but necessary conidition (2.68) does preclude intersections of type (b) shown in Fig. 2.6 from providing stable open-loop working points whereas intersections of type (a) might be stable or unstable. Clearly the likelihood of contravening either condition is increased the larger ΔH, i.e. the more exothermic the reaction, as would be expected.

This possibility of thermal runaway therefore poses a temperature control problem outside the scope of a text on process modelling but its analysis and solution is nevertheless crucial to the formulation of a model for studying the composition control problem.

2.5 Parametric Transfer-Function Matrix Models

We now return to the general problem of obtaining analytical solutions for the behaviour of chemical process plant. Using computer simulation techniques it is, of course, possible to proceed to numerical solutions directly from the system p.d.e's, already derived and the boundary conditions (yet to be considered) without further analysis, given:

(a) a reliable programmer

(b) values for the plant parameters

and (c) a control strategy for adjusting the manipulable input variables.

In practice however what is really required is a method for selecting the parameters and control strategy to produce a loosely pre-specified mode of behaviour of the dependent variables. Posed this way round, computer solution of the problem is no longer direct since numerous iterations of the simulation will be required until the desired parameters and controller structure are, hopefully, determined. With the degrees of freedom possible, rapid convergence to the desired solution is not generally guaranteed.

An analytical model, in the form of a parametric transfer-function matrix (T.F.M), i.e. a T.F.M. where parameters are known functions of plant parameters, is however directly useable by the plant designer and control engineers for the synthesis, in virtually one attempt, of the best plant/controller combination. The accurate derivation of such T.F.M's can be impractically tedious in the completely general case but if the plant possesses certain properties of linearity and symmetry (generally implied by good design as will be seen) such solutions can then be derived. Because of the discrepancies between the plant idealised in this way, and the true system model, simulation is still required but now primed with a rationally determined initial controller structure and initial system parameters from which rapid convergence to the best solution, guided by the insight obtained from the analysed solution, might reasonably be expected.

Likewise, in the field of experimental identification of a difficult process model, analytical solution beforehand of the idealised system, does provide a soundly-based model-structure and good initial values for the iterative parameter-estimation exercise.

The procedure to be followed with spatially-distributed systems of the type examined is broadly as follows, using the liquid/liquid heat exchanger to illustrate the steps involved. It is left to the reader to fill in some of the straightforward manipulations between steps.

2.5.1 Boundary condition formulation

The process description is incomplete without the boundary conditions which must first be determined. In the case of the heat-exchanger these will be taken as being simply

$$\theta_1(o,t) = \text{constant} \tag{2.70}$$

$$\theta_2(L,t) = \text{constant} \tag{2.71}$$

where L is the normalised length of the process.

2.5.2 Large-signal steady-state solution

This is required to provide data for the quasi-constant parameters
of the small signal model and is obtained by setting time-derivatives
to zero in the process p.d.e's, (2.6) in this case, (and d.e's if any)
and solving the resulting spatial d.e.s subject to the boundary conditions,
(2.70) and (2.71) here.   For the symmetrical heat exchanger the solution,
graphed in Fig. 2.7, is

$$\theta_1(h) = \{\theta_1(o)(1+L-h) + \theta_2(L)h\} / (L+1)$$

$$\text{and} \quad \theta_2(h) = \{\theta_1(o)(L-h) + \theta_2(L)(1+h)\}/(L+1)$$

(2.72)

It will be noted from Fig. 2.7 that the two temperature profiles are
separated by a normalised distance of 1.0, i.e. by an actual distance
of L_n the physical significance of which now emerges.   The temperature
profiles have equal constant gradients, which is a special result pertaining
to the summetrically-operated process, producing a constant temperature
drop $\theta_1(h)-\theta_2(h)$ so that heat-transfer is uniformly distributed along
the interface thereby making maximum use of the entire length of the
process i.e. good plant design.

2.5.3 Small-signal model derivation

As with the chemical C.S.T.R. the small-signal equations are derived
from the large-signal equations by implicit differentiation, equating
differentials to small perturbations in the dependent and independent
variables, and substituting steady-state solutions for the coefficient
values.   With spatially distributed processes it is perhaps safer to
operate on the large-signal equations before normalisation since the
base-time, T_n, and base-distance, L_n, may be functions of the variables.
The small-signal equations may then be converted to their simpler normalised
form afterwards.   From large-signal p.d.e's (2.4) we thus obtain

$$\partial\phi_1/\partial\tau = -\partial\phi_1/\partial h + \phi_2 - \phi_1 + f_1(\tau)$$

$$\partial\phi_2/\partial\tau = \partial\phi_2/\partial h + \phi_1 - \phi_2 + f_2(\tau)$$

(2.73)

where flow functions f_1 and f_2 are given by

$$\begin{bmatrix} f_1 \\ f_2 \end{bmatrix} = \frac{\theta_1(o) - \theta_2(L)}{W(L+1)} \begin{bmatrix} 0.6, & -0.4 \\ 0.4, & -0.6 \end{bmatrix} \begin{bmatrix} w_1 \\ w_2 \end{bmatrix}$$

(2.74)

(Had the steady-state gradients $\partial\theta_1/\partial h$ and $\partial\theta_2/\partial h$ not been constant then forcing-functions f_1 and f_2, which involve these gradients, would have been spatially-dependent as well as time-varying so complicating subsequent analysis considerably). The small-signal boundary equations derived from (2.70) and (2.71) in this example are simply

$$\phi_1(o,\tau) = 0 \quad , \quad \phi_2(L,\tau) = 0$$

(2.75)

2.5.4 Laplace transformation with respect to h and

Taking Laplace transforms of the small signal p.d.e's first in p w.r.t. τ and then in s w.r.t. h yields, in this case,

$$p \, \tilde{\tilde{\phi}}_1(s,p) = -(1+s)\tilde{\tilde{\phi}}_1(s,p) + \tilde{\tilde{\phi}}_2(s,p) + \tilde{\phi}_1(o.p) + s^{-1}\tilde{f}_1(p)$$

$$p \, \tilde{\tilde{\phi}}_2(s,p) = -(1-s)\tilde{\tilde{\phi}}_2(s,p) + \tilde{\tilde{\phi}}_1(s,p) - \tilde{\phi}_2(o,p) + s^{-1}\tilde{f}_2(p)$$

(2.76)

(for zero initial conditions), in which superscript $\tilde{}$ denotes transforms w.r.t h and τ and $\sim$ w.r.t τ only. Boundary conditions specified at h = 0 can be eliminated at this stage, here by simply putting $\tilde{\phi}_1(o,p)$ to zero as demanded by (2.75) but $\tilde{\phi}_2(o,p)$ is present unknown and must therefore be retained until after inversion back to the space domain.

2.5.5 Inversion to the h,p domain

Having isolated separate expressions from (2.76) for $\tilde{\tilde{\phi}}_1(s,p)$ and $\tilde{\tilde{\phi}}_2(s,p)$ in terms of inputs $\tilde{f}_1(p)$, $\tilde{f}_2(p)$ and the unknown $\tilde{\phi}_2(o,p)$ these may now be inverted from the s,p to the h,p domain with the aid of Laplace

transform tables and, by substituting L=h, the second boundary condition

of (2.75) may be invoked to yield an expression for $\tilde{\phi}_2(o,p)$ which may

then be used to determine $\tilde{\phi}_1(L,p)$. These two results grouped into

matrix form are conveniently expressed thus:

$$\begin{bmatrix} \tilde{\phi}_1(L,p) - \tilde{\phi}_2(o,p) \\ \\ \tilde{\phi}_1(L,p) + \tilde{\phi}_2(o,p) \end{bmatrix} = \{ \frac{\theta_1(o) - \theta_2(L)}{W(L+1)} \} \ \underline{G}(p) \begin{bmatrix} \tilde{w}_1(p) + \tilde{w}_2(p) \\ \\ \tilde{w}_1(p) - \tilde{w}_2(p) \end{bmatrix} \quad (2.77)$$

where the T.F.M., $\underline{G}(p)$ takes the diagonal form

$$\underline{G}(p) = \begin{bmatrix} g_1(p) \ , \ o \\ \\ o \ , \ g_2(p) \end{bmatrix} \quad (2.78)$$

where

$$g_1(p) = \frac{0.2\{ p(\cosh qL-1)+q \ \sinh \ qL\}}{q \ \{q \ \cosh \ qL + (1+p) \ \sinh \ qL\}} \quad (2.79)$$

and

$$g_2(p) = \frac{(q^2/p)(\cosh qL-1)+q \ \sinh \ qL}{q\{q \ \cosh \ qL+(1+p) \ \sinh \ qL\}} \quad (2.80)$$

the frequency function q being given by

$$q^2 = p(p+2) \quad (2.81)$$

Alternatively, in terms of the real life input and output vectors,

rather than their so called "tilt" and "total" combinations (2.77) may

be expressed:

$$\begin{bmatrix} \tilde{\phi}_1(L,p) \\ \\ \tilde{\phi}_2(0,p) \end{bmatrix} = \{ \frac{\theta_1(o)-\theta_2(L)}{2W(L+1)} \} \begin{bmatrix} 1 \ , \ 1 \\ \\ -1 \ , \ 1 \end{bmatrix} \begin{bmatrix} g_1(p) \ , \ 0 \\ \\ o \ , \ g_2(p) \end{bmatrix} \begin{bmatrix} 1 \ , \ 1 \\ \\ 1 \ , \ -1 \end{bmatrix} \begin{bmatrix} \tilde{w}_1(p) \\ \\ \tilde{w}_2(p) \end{bmatrix} \quad (2.82)$$

the T.F.M. between this input and output vector having a "Dyadic"

structure[6] because the dynamics of the system are contained entirely

within a diagonal matrix that is coupled to the observed outputs and

manipulable inputs by purely static matrices. This structure arises

from the physical symmetry of the process considered and occurs frequently

in analytically-derived T.F.M. models because tractable analytic solutions

are generally limited to symmetrical cases – as has been already emphasised.   Since control system design lies outside the scope of this text suffice it to note that the dyadic nature of system's T.F.M. clearly makes the solution of the interaction problem in controller design a fairly trivial exercise exhaustively investigated by Owens[6], (who has also considered the application of Dyadic approximation which would be applicable to plants operated with a degree of assymmetry).   The problem therefore reduces essentially to the design of stable controllers for the individual diagonal terms of $\underline{G}(p)$, the computed inverse Nyquist loci for which are shown in Figs. 2.8 and 2.9 for the case of L=2.0.   These are clearly directly useable for control system synthesis.

Approximations to $g_1(p)$ and $g_2(p)$ may also be derived (a) by simplification of their accurate formulae (2.79) and (2.80) to provide a check on the computation of the true loci or (b) directly from the small-signal p.d.e's and boundary conditions to avoid the labour of deriving precise solutions altogether.   The approach resembles in some respects those of Owens[7] and Friedly[8] and involves the matching of asymptotic models derived for very-high and very-low ranges of frequency.

2.5.6 Multivariable first-order lag models

Owens[7] has proposed that if a system has an inverse T.F.M. $\underline{G}*(p)$ where

$$\lim_{p \to \infty} p^{-1} \underline{G}*(p) = \underline{A}_0 \tag{2.83}$$

$$\text{and } \lim_{p \to 0} \underline{G}*(p) = \underline{A}_1 \tag{2.84}$$

where $\underline{A}_0$ and $\underline{A}_1$ are constant matrices then, under certain conditions, $\underline{G}*(p)$ may be approximated, for controller design purposes, by a multivariable first-order lag system of inverse T.F.M. $\underline{G}_A*(p)$ where

$$\underline{G}_A{}^*(p) = \underline{A}_1 + \underline{A}_o p \qquad (2.85)$$

since $G^*(p)$ and $G_A{}^*(p)$ approach equality at very-high and very-low

frequencies. Such a representation is highly appropriate and very

convenient in chemical plant modelling since $\underline{A}_1$ and $\underline{A}_o$ are readily

determined either from measurements of the initial rates and the

settling values of the system's step responses or by simple analytical

derivation. From the transformed system p.d.e's (2.76) in this

example $\underline{A}_1$ is readily deduced by merely ignoring all dependent variables

other than those with coefficients involving the highest power of p.

In this case clearly we get

$$\lim_{p \to \infty} p \begin{bmatrix} \tilde{\phi}_1(h,p) \\ \tilde{\phi}_2(h,p) \end{bmatrix} = \begin{bmatrix} \tilde{f}_1(p) \\ \tilde{f}_2(p) \end{bmatrix} \qquad (2.86)$$

from which, transforming to our tilt and total variables we get

$$\lim_{p \to \infty} p \begin{bmatrix} \tilde{\phi}_1(L,p) - \tilde{\phi}_2(0,p) \\ \tilde{\phi}_1(L,p) + \tilde{\phi}_2(0,p) \end{bmatrix} = \left\{ \frac{\theta_1(o) - \theta_2(L)}{W(L+1)} \right\} \begin{bmatrix} 0.2 & , & 0 \\ 0 & , & 1 \end{bmatrix} \begin{bmatrix} \tilde{w}_1(p) + \tilde{w}_2(p) \\ \tilde{w}_1(p) - \tilde{w}_2(p) \end{bmatrix} \qquad (2.87)$$

from which matrix $\underline{A}_o$ is immediately obtainable. It is interesting to

note that $\underline{A}_o$ is spatially-independent and independent of boundary conditions

upon which $\underline{A}_1$ is crucially dependent. $\underline{A}_1$ is in fact determined by the

solution of the small-signal p.d.e's (2.73) with constant inputs subject

to the system boundary conditions (2.75) in this example with time-

derivatives set to zero. In the case of the heat-exchanger this yields

the result

$$\begin{bmatrix} \phi_1(L) - \phi_2(0) \\ \phi_1(L) + \phi_2(0) \end{bmatrix} = \left\{ \frac{\theta_1(o) - \theta_2(L)}{W(L+1)} \right\} \begin{bmatrix} 0.2L/(L+1) & , & 0 \\ 0, & L \, . \end{bmatrix} \begin{bmatrix} w_1 + w_2 \\ w_1 - w_2 \end{bmatrix} \qquad (2.88)$$

From (2.87) and (2.88) we therefore deduce that the multivariable

first-order lag model for the system to be

$$
\begin{bmatrix} \tilde{\phi}_1(L,p)-\tilde{\phi}_2(o,p) \\ \tilde{\phi}_1(L,p)+\tilde{\phi}_2(o,p) \end{bmatrix} \simeq \frac{\theta_1(o)-\theta_2(L)}{W(L+1)} \begin{bmatrix} 0.2\{(L+1)/L+p\}^{-1} & , & 0 \\ & & \\ 0 & , & (1/L+p)^{-1} \end{bmatrix} \begin{bmatrix} \tilde{w}_1(p)+\tilde{w}_2(p) \\ \tilde{w}_1(p)-\tilde{w}_2(p) \end{bmatrix}
$$

(2.89)

the inverse Nyquist loci for which are also shown in Figs. 2.8 and

2.9, for L=2.0, alongside the true system loci. Agreement is clearly

good but the loops in the true loci could produce unexpected oscillation

or even instability in the presence of high-gain integral control action.

2.5.7 Lag/delay models

Failure to predict the loops in the inverse Nyquist loci arises

from neglecting the imaginary nature of p when considering the high-

frequency asymptotic behaviour of the system. If therefore only the

interactive terms are omitted from (2.76) (rather than all dependent

variables not multiplied by p) we obtain, since $\phi_1(o,p) = 0$,

$$
\tilde{\tilde{\phi}}_1(s,p) = f_1(p)/s(s+p+1)
$$

and (2.90)

$$
\tilde{\tilde{\phi}}_2(s,p) = \{\tilde{\phi}_2(o,p) - \tilde{f}_2(p)/s\}/\{s-(p+1)\}
$$

giving, an inversion and substituting h=L, , $\left\{ \text{since } \tilde{\phi}_2(L,p)=0 \right\}$,

$$
\begin{bmatrix} \tilde{\phi}_1(L,p) \\ \\ \tilde{\phi}_2(O,p) \end{bmatrix} = \frac{1-\exp\{-(p+1)L\}}{(p+1)} \begin{bmatrix} \tilde{f}_1(p) \\ \\ \tilde{f}_2(p) \end{bmatrix}
$$

(2.91)

Now substituting for $\tilde{f}_1(p)$ and $\tilde{f}_2(p)$ in terms of $\tilde{w}_1(p)$ and $\tilde{w}_2(p)$ we

obtain the high-frequency model:

$$\underset{|p| \to \infty}{\text{Lim}} \left(\frac{p}{1-\exp\{-(p+1)L\}} \right) \begin{pmatrix} \tilde{\phi}_1(L,p)-\tilde{\phi}_2(o,p) \\ \tilde{\phi}_1(L,p)+\tilde{\phi}_2(o,p) \end{pmatrix} = \{\frac{\theta_1(o)-\theta_2(L)}{W(L+1)}\} \begin{pmatrix} 0.2, & 0 \\ 0 & ,1.0 \end{pmatrix} \begin{pmatrix} \tilde{w}_1(p)+\tilde{w}_2(p) \\ \tilde{w}_1(p)-\tilde{w}_2(p) \end{pmatrix}$$

$$(2.92)$$

which resembles the high-frequency equation (2.87) apart from the appearance

of the attenuated delay-term $\exp\{-(p+1)L\}$ and the indication that the limit

applies irrespective of p being real or complex. The same result may be

derived from the accurate model (2.77) to (2.81) noting that, as $|p| \to \infty$,

$$q \to p + 1.0 \qquad\qquad (2.93)$$

Combining the inverse system T.F.M's for low and high-frequency in a manner

similar to that for first-order lag approximation we therefore now obtain the

multivariable lag/delay model:

$$\begin{pmatrix} \tilde{\phi}_1(L,p)-\tilde{\phi}_2(o,p) \\ \tilde{\phi}_1(L,p)+\tilde{\phi}_2(o,p) \end{pmatrix} \approx \frac{\theta_1(o)-\theta_2(L)}{W(L+1)} \begin{pmatrix} 0.2\left[\frac{(L+1)}{L} + \frac{p}{1-\exp\{-(p+1)L\}}\right]^{-1}, & 0 \\ 0, & \left[\frac{1}{L} + \frac{p}{1-\exp\{-(p+1)L\}}\right]^{-1} \end{pmatrix} \begin{pmatrix} w_1(p) + w_2(p) \\ w_1(p) - w_2(p) \end{pmatrix}$$

$$(2.94)$$

which exhibits loops in its inverse Nyquist loci very similar to those of the

real system as inspection of Figs. 2.8 and 2.9 reveals.

The loops are in fact the result of reflected travelling waves in the

process which become progressively more attenuated with the passage of time.

The first-order lag model predicts only the fundamental integrating nature

of the system at high-frequency whilst the lag-delay model reproduces the

effect of the passage of the first of these waves in addition.

The analytical approach to T.F.M. development outlined in this Section

is next applied to the distillation process described earlier. This is a

much more difficult case because of, (a), its two-stage construction,

therefore involving four boundaries not two and (b), the relative complexity

of the individual boundary equations. Solution is however not impossibly

tedious if full advantage is taken of physical symmetry to simplify the

system equations at every step of the analysis. Because of space limitations

only the key intermediate results are provided here but the reader should
not have great difficulty in performing the intermediate manipulations for
himself. The fully worked-out analyses are to be found in references
(9)(10) and (11).

2.6 The Analytical Determination of Parametric T.F.M's for Symmetrical
Distillation Columns.

2.6.1 Large-signal boundary conditions

Without these the system description is incomplete and their formulation
requires the consideration of the mass balances pertaining at the top and
bottom of both the rectifier and stripping sections. Their final forms differ
somewhat in the cases of packed and tray-type columns largely because of the
fixed, finite cell-length in the latter case. Considering the feed point,
firstly for packed columns it is readily deduced that, for the vapour and
liquid streams respectively:

$$V_s \, Y'(o) + F_v z = V_r \, Y(o) \qquad \Big\}$$

$$\text{and} \qquad L_r \, X(o) + F_\ell Z = L_s X'(o) \qquad \Big\} \qquad (2.95)$$

and it follows from the assumed symmetry conditions (2.21) that the liquid
and vapour feed flows must be equal and given by

$$F_v = F_\ell \triangleq F = V \, \epsilon / \alpha \qquad (2.96)$$

where $\qquad \epsilon = \alpha - 1 \qquad (2.97)$

For symmetry we shall also assume that the feed mixture is supplied in
equilibrium <u>for both sections</u> so that

$$z = \alpha \, Z \quad \text{and} \quad z = 1 - Z \qquad (2.98)$$

so fixing z and Z to fixed nominal working values. For the tray column
however considering the tray above the feed point we deduce that

$$H_\ell \, \delta h \, dX(o)/dt = Fz + V_s Y'(o) - V_r Y(o) + L_r \{X(1) - X(o)\}$$

so that approximating the finite difference in X by the first spatial
derivative, eliminating X and Y' in favour of Y and X', substituting for
z and normalising we get

$$\partial Y(o)/\partial \tau = -2/(\alpha+1) + X'(o) + \{1-Y(o)\} + \partial Y(o)/\partial h \qquad (2.100)$$

and similarly for the tray beneath the feed point

$$\partial X'(o)/\partial \tau = 2/\alpha+1) - X'(o) - \{1-Y(o)\} - \partial X'(o)/\partial h \qquad (2.101)$$

Turning attention now to the top - (accumulator) end of the rectifier (h=L)
we have, for the packed-column

$$H_e \ dX(L)/dt = V_r Y(L) - V_r X(L) \qquad (2.102)$$

where H_e is the capacitance of the accumulator. Assuming this vessel to
run in continuous equilibrium therefore

$$H_e \ \alpha \quad dY_e(L)/dt = V_r\left[\alpha\{1 - Y_e(L)\} - \{1 - Y(L)\}\right] \qquad (2.103)$$

Similar consideration applied to the reboiler (h = -L) give

$$H_e \ \alpha \quad dX'_e(L)/dt = L_s\left[X'(-L) -\alpha \ X'_e(-L)\right] \qquad (2.104)$$

if $\alpha \ H_e$ is the reboiler capacitance. The tray-column's terminal conditions
are similar in their finite difference form i.e. for the accumulator:

$$H_e \ dX(N+1)/dt = V_r \ \{Y(N) - X(N+1)\} \qquad (2.105)$$

but $\qquad X(N+1) \simeq X(N) +\{\partial X(N)/\partial h'\}\delta h' \qquad (2.106)$

so that eliminating X in favour of Y using the equilibrium relationship
(2.13) a normalising yields.

$$T_e\partial \ Y(L)/\partial \tau = \varepsilon\{1-Y(L)\} - \partial Y(L)/\partial h \qquad (2.107)$$

and similarly for the reboiler

$$T_e \ \partial X'(-L)/\partial \tau = - \ \varepsilon X'(-L) + \ \partial X'(-L)/\partial h \qquad (2.108)$$

where T_e is the normalised time-constant of the end-vessels given by

$$T_e = H_e/H \ \delta h' \qquad (2.109)$$

2.6.2 Large-signal steady-state solution

With the formulation of the four boundary conditions the two columns
are now completely specified and steady-state solutions for constant inputs
$(V_r, L_r, F_v, F_\ell, Z$ and $z)$ may be determined by the simultaneous solution of
p.d.e's (2.22),(2.23) with (2.95) (2.103),(2.104) for the packed column
and p.d.e's (2.31) with (2.100),(2.101),(2.107) and (2.108) for the tray

column, putting the time-derivatives to zero beforehand. Because of the

symmetry of the system equations resulting from operating at flow condi-

tions(2.2.1) and with input compositions governed by (2.98) the composition

profiles $Y(h)$, $Y_e(h)$, $X'(h)$ and $X_e'(h)$ are readily determined and are found

to be linear. The solutions are graphed in Fig. 2.10 in which G is the

composition gradient given by

$$G = 2 \ \varepsilon/(\alpha+1)(2 \ \varepsilon L + \alpha+1) \qquad (2.110)$$

The equal separation per unit length of column is again characteristic of a

well-designed plant making full use of the available column volume. Solutions

$Y(h)$ and $X'(h)$ for the tray-column are found to be identical to those for.

$Y_e(h)$ and $X_e'(h)$ in the packed column because of the continuous equilibrium

assumption. The equality of $X'(-h)$ and $1-Y(h)$ and if $X_e'(-h)$ and $1-Y_e(h)$ is

an important symmetrical property of these profiles which also greatly eases

solution of the small-signal model now to be considered.

2.6.3 Small signal p.d.e's and Laplace transformation

2.6.3.1 Reversal of rectifier distance base

It will be recalled from the heat-exchanger case that the first dependent

variable to emerge from the solution was $\tilde{\phi}_2(o,p)$ from which $\tilde{\phi}_1(L,p)$ and

indeed $\tilde{\phi}_1(h,p)$ and $\tilde{\phi}_2(h,p)$ could then be obtained by substitution of the

$\tilde{\phi}_2(o.p)$ expression. The important dependent variables in the column are

the output perturbations $y(L)$ and $x'(-L)$ in $Y(L)$ and $X'(L)$ and labour is

therefore saved if these too emerge first form the analysis so saving addi-

tional substitution of perhaps complex expressions. The distance base is

therefore now altered replacing h by L-h in the rectifier equations and h

by L+h in the stripper equations, so that h = L now locates the feed point

in both cases and h = o locates the top and bottom of the entire column.

$y(L)$ and $x'(-L)$ in the original system of coordinates therefore now become

$y(o)$ and $x'(o)$ whilst $y(o)$ and $x'(o)$ in the original base now become $y(L)$

and $x'(L)$. The transformation is best understood by imagining the column bent into an inverted U-tube with the feed-point now at the top of the U and both the reboiler <u>and</u> accumulator now at the bottom. The transformation clearly reverses the sign of the odd but not the even-spatial derivatives in the rectifier equations. The new base is assumed in all subsequent equations.

By implicit differentiation of the general packed column p.d.e's (2.18) and (2.19) and substitution of the symmetrical steady-state solutions we get, after normalising,

$$c\partial y/\partial \tau - \partial y/\partial h + G\, v/V = y_e - y$$
$$- \partial y_e/\partial \tau - \partial y_e/\partial h + \alpha\, G\, \ell/V = y_e - y$$
$$- \partial x'/\partial \tau + \partial x'/\partial h + G\ell/V = x' - x_e'$$
$$c\partial x_e'/\partial \tau + \partial x'_e/\partial h + \alpha\, G\, v/V = x' - x_e' \qquad (2.111)$$

in which v and ℓ denote perturbations in inputs V_r and L_r, whilst the boundary conditions (2.45), (2.103) and (2.104) yield, (in the new base),

$$y(L) = x_e'(L) - (\epsilon/2)G\, v/V$$
$$x'(L) = y_e(L) + (\epsilon/2)G\, \ell/V \qquad (2.112)$$

$$\alpha(1 + T\, \partial/\partial \tau)\, y_e(o) = y(o)$$
and
$$\alpha(1 + T\, \partial/\partial \tau)x'_e(o) = x'(o) \qquad (2.113)$$

Taking Lapalce transforms of the p.d.e's in s w.r.t. h and in p w.r.t τ produces

$$(1 + cp - s)\tilde{\tilde{y}} - \tilde{\tilde{y}}_e + G\tilde{v}/Vs + \tilde{y}(o) = 0$$
$$-(1+p+s)\, \tilde{\tilde{y}}_e + \tilde{\tilde{y}} + \alpha\, G\, \tilde{\ell}/Vs + \tilde{y}_e(o) = 0$$
$$-(1+p-s)\, \tilde{\tilde{x}}' + \tilde{\tilde{x}}_e' + G\, \tilde{\ell}/Vs - \tilde{x}'(o) = 0$$
$$(1 + cp + s)\, \tilde{\tilde{x}}_e' - \tilde{\tilde{x}}' + \alpha\, G\, \tilde{v}/Vs - \tilde{x}_e'(o) = 0 \qquad (2.114)$$

whilst transforming (2.113) w.r.t τ only gives

$$\tilde{\tilde{y}}_e(o) = \alpha^{-1}h_e(p)\, \tilde{y}(o)$$
$$\tilde{\tilde{x}}_e(o) = \alpha^{-1}h_e(p)\, x'(o) \qquad (2.115)$$

where $h_e(p)$ is the transfer function of the end vessels, i.e.

$$h_e(p) = 1/(1 + T\, p) \qquad (2.116)$$

The system clearly becomes completely symmetrical if we set c, the column's vapour/liquid capacitance ratio, = 1.0[†] producing both dynamic as well as static symmetry.

2.6.4 Matrix representation

Adding and subtracting the analogous equations of set (2.114) produces equations in composition $\underline{tilts}$ and $\underline{totals}$ resembling their temperature equivalents in Section 2.5. Furthermore identical coefficients appear in the resulting equations so yielding matrix equations with purely diagonal coefficient matrices which greatly assists solution. In particular, if input and output vectors are defined thus

$$\underline{q} = \begin{bmatrix} y - x' \\ y + x' \end{bmatrix} \; , \; \underline{r} = \begin{bmatrix} y_e - x_e' \\ y_e + x_e' \end{bmatrix} \text{ and } \underline{u} = \frac{G}{V} \begin{bmatrix} v + \ell \\ v - \ell \end{bmatrix} \tag{2.117}$$

we get $(1 + p - s) \; \underset{\sim}{\tilde{q}} - \underset{\sim}{\tilde{r}} = - \; s^{-1} \; \underset{\sim}{\tilde{u}} - \underset{\sim}{\tilde{q}}(o)$

and

$$-(1+p+s)\underset{\sim}{\tilde{r}} + \underset{\sim}{\tilde{q}} = \alpha \; s^{-1} \begin{bmatrix} -1 \; , \; 0 \\ 0 \; , \; 1 \end{bmatrix} \; \underset{\sim}{\tilde{u}} - \underset{\sim}{\tilde{r}}(o) \tag{2.118}$$

whilst similar operations on the boundary conditions (2.112) and (2.115) produce:

$$\underline{q}(L) = \begin{bmatrix} -1 \; , \; 0 \\ 0 \; , \; 1 \end{bmatrix} \; \underline{r}(L) - \frac{\varepsilon}{2} \; \underline{u} \tag{2.119}$$

and

$$\underset{\sim}{\tilde{r}}(o) = \alpha^{-1} \; h_e(p) \; \underset{\sim}{\tilde{q}}(o) \tag{2.120}$$

2.6.5 Inversion to the h,p domain

Again the boundary conditions at h = 0 {equation 2.120} may be used immediately to eliminate say the unknown $\underset{\sim}{\tilde{r}}(o)$ from the transformed p.d.e's which may then be manipulated and inverted before substituting the second pair of boundary conditions for h = L (2.119) so yielding the desired solution for $\tilde{q}(o,p)$, and hence for y(o,p) and x'(o,p). This is found to be

[†]This assumption implies high pressure distillation. It is not essential to the tractability of the solution but is helpful in as much as it produces diagonal coefficient matrices.

$$\tilde{q}(o,p) = \begin{bmatrix} g_1(o,p) & , & 0 \\ 0 & , & g_2(o,p) \end{bmatrix} \tilde{u}(p) \qquad (2.121)$$

where $g_1(o,p) = \dfrac{\{\varepsilon(\cosh q\,L - 1)/p - (1+\alpha)(\sinh q\,L)/q - \varepsilon/2}{\{(1 - h_e\,\alpha^{-1})(\sinh q\,L)q/p + (1 + h_e\alpha^{-1})\cosh q\,L\}} \qquad (2.122)$

and
$$g_2(o,p) = \frac{\{\varepsilon p(\cosh q\,L - 1)/q^2 - (\alpha+1)(\sinh q\,L)/q - \varepsilon/2\}}{\{(1 + h_e\alpha^{-1})(\sinh q\,L)p/q + (1 - h_e\alpha^{-1})\cosh q\,L\}} \qquad (2.123)$$

where again $q^2 = p(p + 2)$ $\qquad (2.124)$

and, for zero-frequency, i.e. step inputs

$$g_1(o,o) = \alpha\{\varepsilon\,L^2 - (\alpha+1)L - \varepsilon/2\} \,/\, \{2\varepsilon L + \alpha + 1\} \qquad (2.125)$$

and

$$g_2(o,o) = -\ \alpha\{(\alpha + 1)L + \varepsilon/2\}/\varepsilon \qquad (2.126)$$

Of course these results apply to the packed-column but an analysis of the tray-column may be carried out on lines[*] similar to those demonstrated in Section 2.6.3 to 2.6.5 producing a result as (2.121) but in which the elements are here given by slightly different formulae, viz.

$$g_1(o,p) = \frac{\varepsilon\{(p+2)(\cosh\sqrt{p}L - 1)/p + (\sinh\sqrt{p}L)/\sqrt{p} + 0.5\}}{\{(1 + T)p + 2 + \varepsilon\}\cosh\sqrt{p}\,L + \{(p+2)(\varepsilon+Tp) + p\}(\sinh\sqrt{p}L)/\sqrt{p}} \qquad (2.127)$$

$$g_2(o,p) = -\ \frac{(\alpha+1)(\cosh\sqrt{p}L - 1) + (\alpha+1)\sinh\sqrt{p}\,L/\sqrt{p} + 0.5\,(3\alpha + 1)}{\{p(1+T) + \varepsilon\}\cosh\sqrt{p}\,L + \sqrt{p}(1+\varepsilon+Tp)\sinh\sqrt{p}\,L} \qquad (2.128)$$

$$g_1(o,o) = (\varepsilon L^2 + \alpha + 1)/(2\varepsilon L + \alpha + 1) \qquad (2.129)$$

and

$$g_2(o,o) = -\ \{(\alpha+1)L + 0.5\,(3\alpha + 1)\}/\,\varepsilon \qquad (2.130)$$

2.6.4 Form of the inverse Nyquist loci

Two examples, for packed-columns, of the behaviour $g_1(o,j\omega)^{-1}$ are illustrated in Fig. 2.11 for the following parameters

[*] Although vector $\underline{r}$ as defined in (2.117) will not appear in this case, the double spatial derivative of q will also generate two unknown vectors at $h = o$ upon transforming the system p.d.e's, so again requiring two sets of boundary conditions.

(a) $\varepsilon = 0.75$, $(\alpha = 1.75)$, $L = 2.8$, $T = 20$

and (b) $\varepsilon = 1.0$, $(\alpha = 2.0)$, $L = 5.0$, $T = 20$

In both cases loops due to travelling wave effects are clearly visible and obviously of greater significance in the case of the shorter column (a) which, as might be expected, causes less attenuation of the waves between reflections. It is also very important, however, to note that the sign of the static gain $g_1(o,o)$ is parameter-dependent, being positive for longer columns or, more precisely, if

$$\varepsilon L^2 > (\alpha + 1)L + \varepsilon/2 \tag{2.131}$$

whereas, over higher frequency ranges, the gain is invariably negative. Larger columns of the packed-type therefore produce non-minimum-phase open-loop behaviour (and therefore severe closed-loop stability constraints) as indicated by the encirclement of the origin by locus (b), which would not be predicted by say, first-order lag modelling, based on equation (2.85) due to the opposing signs of corresponding elements of matrices $\underline{A}_1$ and $\underline{A}_o$.

{The true loci are compared in Fig. 2.11 with their multivariable first-order lag approximations derived from (2.125) and the approximate high-frequency model

$$\underset{p \to \infty}{\text{Lim}} \quad p \, \tilde{\underline{q}} = - \, \tilde{\underline{u}} \tag{2.132}$$

obtained from the first equation of (2.118)}

First-order lag modelling is, however, applicable to tray-columns[12,13], the high-and low-frequency gains of which are of identical sign* (positive for $g_1(o,p)$ and negative for $g_2(o,p)$). Travelling-wave effects are here found to be unimportant because the validity of the spatially-continuous model for tray columns depends upon L being $\gg 1$. In the case of shorter packed columns i.e. those not satisfying (2.131) first-order lag modelling

* Rosenbrock[14] in 1966 first indicated the possibility of important behavioural differences between packed and tray-type columns resulting from the basic differences in their p.d.e's. It has nevertheless taken until now for these differences to be identified thoroughly[9,10,11,15] probably because of the avoidance of the analytical approach by the majority of researchers.

may also be applied but here the additional phase lag caused by the signifi-
cant wave effects must also be included for high gain controller design.

2.7 Discussion

In chapter 5 it has been demonstrated that, by using elementary physical
and chemical balance and equilibrium concepts, idealised units of chemical
process plant, involving significant spatial variation, can be modelled by
partial differential equations (p.d.e's) of similar type, involving only
first-order derivatives in space (h) and time (τ), whether the dominant
phenomenon is material-transfer, heat-transfer or chemical-change. It has
been shown that physically-discretised processes involving numerous
stirred tanks can also be represented approximately by p.d.e's involving
second-order spatial derivatives. The analytical determination of parametric
transfer-function matrices (T.F.M's) has been demonstrated involving the
following sequence of steps

    (a)   boundary condition formulation

    (b)   large signal steady-state solution

    (c)   derivation of the small signal p.d.e's and boundary conditions

    (d)   double Laplace transformation

    (e)   substitution of known boundary conditions (at h = o)

    (f)   inversion of transformed system to the space-frequency domain

and (g)   substitution of remaining boundary conditions (at h = L)

Analytical solution does demand a high degree of symmetry and linearity
in the plant equations but fortunately this is also a characteristic of good
plant design. The symmetry leads to T.F.M.'s of Dyadic structure the control
design for which is much more straightforward than for multivariable systems
in general because of the ease with which interaction can be removed.

The examples considered have revealed that the fundamental high-frequency
behaviour is dictated by the p.d.e's alone whereas boundary conditions domi-
nate low-frequency behaviour. Because of the very diverse range of boundary

conditions possible from process to process therefore, very different overall dynamic behaviour can be expected from processes governed by similar p.d.e's including non-minimum-phase responses. Travelling-wave phenomena can be important in processes of length insufficient to cause significant attenuation between wave reflections and in such circumstances lag/delay models can closely reproduce true system behaviour. In other circumstances multivariable first-order lag approximations provide rapid approximate solutions provided high-and low-frequency gains are of identical sign i.e. provided the system is of a minimum-phase type.

The Chapter has been restricted to processes involving one dominant physical or chemical phenomenon though it has been demonstrated that chemical/thermal interactions can in practice demand the consideration of these two effects simultaneously. The analytical solution of the idealised decomposed system can nevertheless provide, in general, good initial parameter values and controller strategies with which to begin detailed computer or pilot-plant simulations.

2.8 References

(1) Judson King, C., 'Separation Processes', 1971, (New York: McGraw Hill).

(2) Wilkinson, W.L., and Armstrong, W.D., Chem. Eng. Sci., 1957, 7, No. 1/2.

(3) Rademaker, O., Rijnsdorp, J.E. and Maarleveld, A., 'Dynamics and control of continuous distillation units', 1975, (Amsterdam:Elsevier).

(4) Denbigh, K. and Turner, J.C.R., 'Chemical reactor theory', 1973, (Cambridge University Press).

(5) Himmelblau, D.M. and Bischoff, K.B., 'Process analysis and simulation - Deterministic systems', 1968, (New York: J. Wiley and Son).

(6) Owens, D.H., 'Dyadic expansions and their applications', Proc. IEE, Vol. 126, No. 6, 1979, pp. 563-567.

(7) Owens, D.H., 'Feedback and multivariable systems', IEE Control Engineering Series 7, 1978 (London: Peter Peregrinus)

(8) Friedly, J.C., 'Asymptotic approximations to plug flow process dynamics', A.I.Ch.E., June 1967.

(9)   Edwards, J.B., 'The analytical modelling and dynamic behaviour of a
      spatially continuous binary distillation column', University of
      Sheffield, Dept. of Control Engineering, Research Report No. 86,
      April 1979.

10)   Edwards, J.B., 'The analytical modelling and dynamic behaviour of
      tray-type beinary distillation columns', ibid, Research Report No. 90,
      June 1979.

11)   Edwards, J.B., 'The analytical determination of the composition
      dynamics of binary distillation columns of the packed-and tray-type'.
      Trans. Instn., Chem., Engrs.,: to be published.

12)   Edwards, J.B. and Jassim, H.J., 'An analytical study of the dynamics
      of binary distillation columns', Trans. Instn. Chem. Engrs., Vol. 55,
      1977, pp. 17-28.

13)   Edwards, J.B., and Owens, D.H., "First-order type models for multi-
      variable process control", Proc. IEE, 1977, 124, (11), pp. 1083-1088.

14)   Rosenbrock, H.H., and Storey, C., 'Computational techniques for
      Chemical Engineers', 1966, (London:Pergamon Press).

15)   Edwards, J.B., 'The dynamic behaviour of packed and tray-type binary
      distillation columns described by lumped parameter models', University
      Of Sheffield, Dept. of Control Engineering, Research Report No. 91,
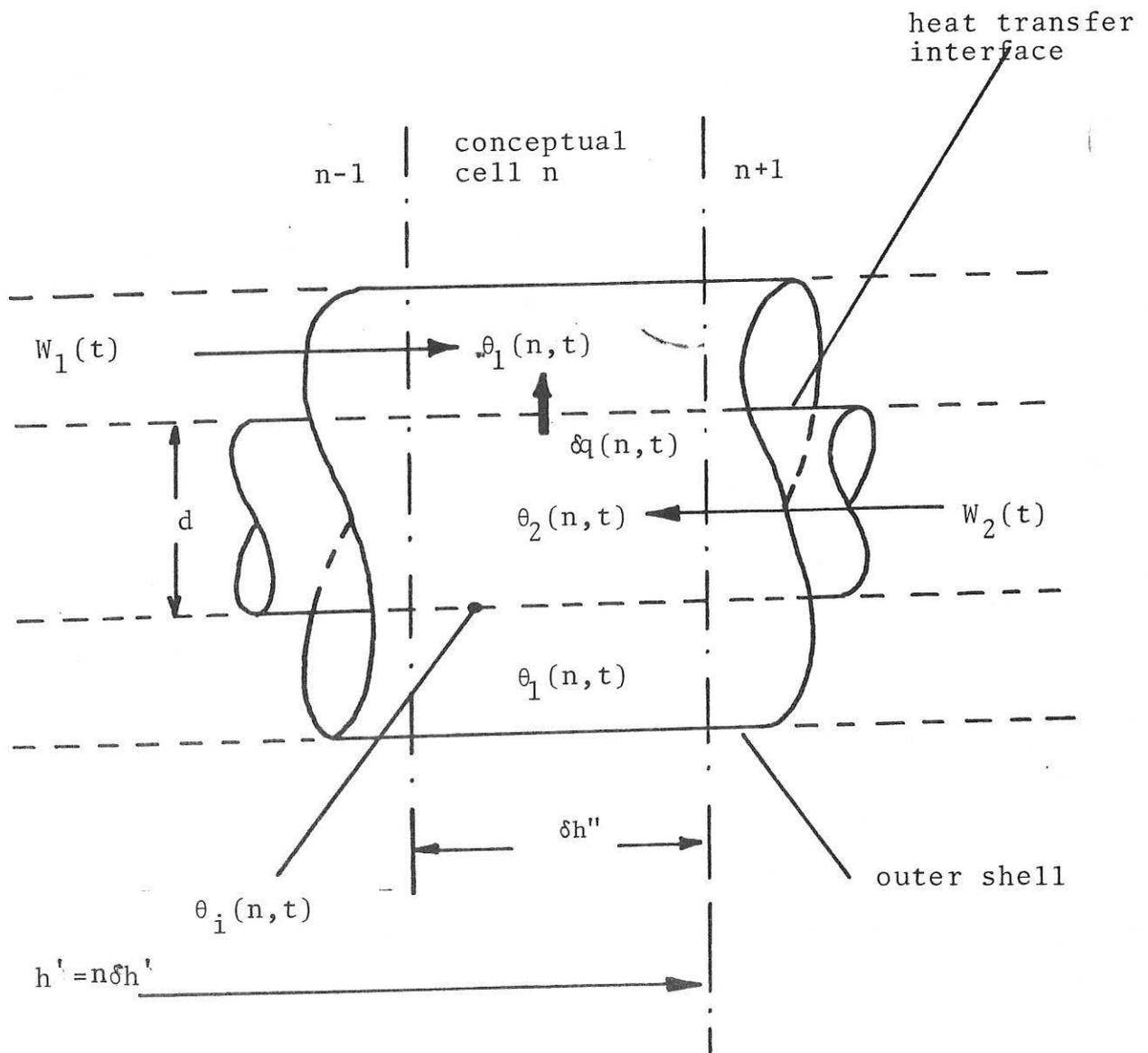   June 1979.

Fig. 2.1   Variables associated with n'th cell
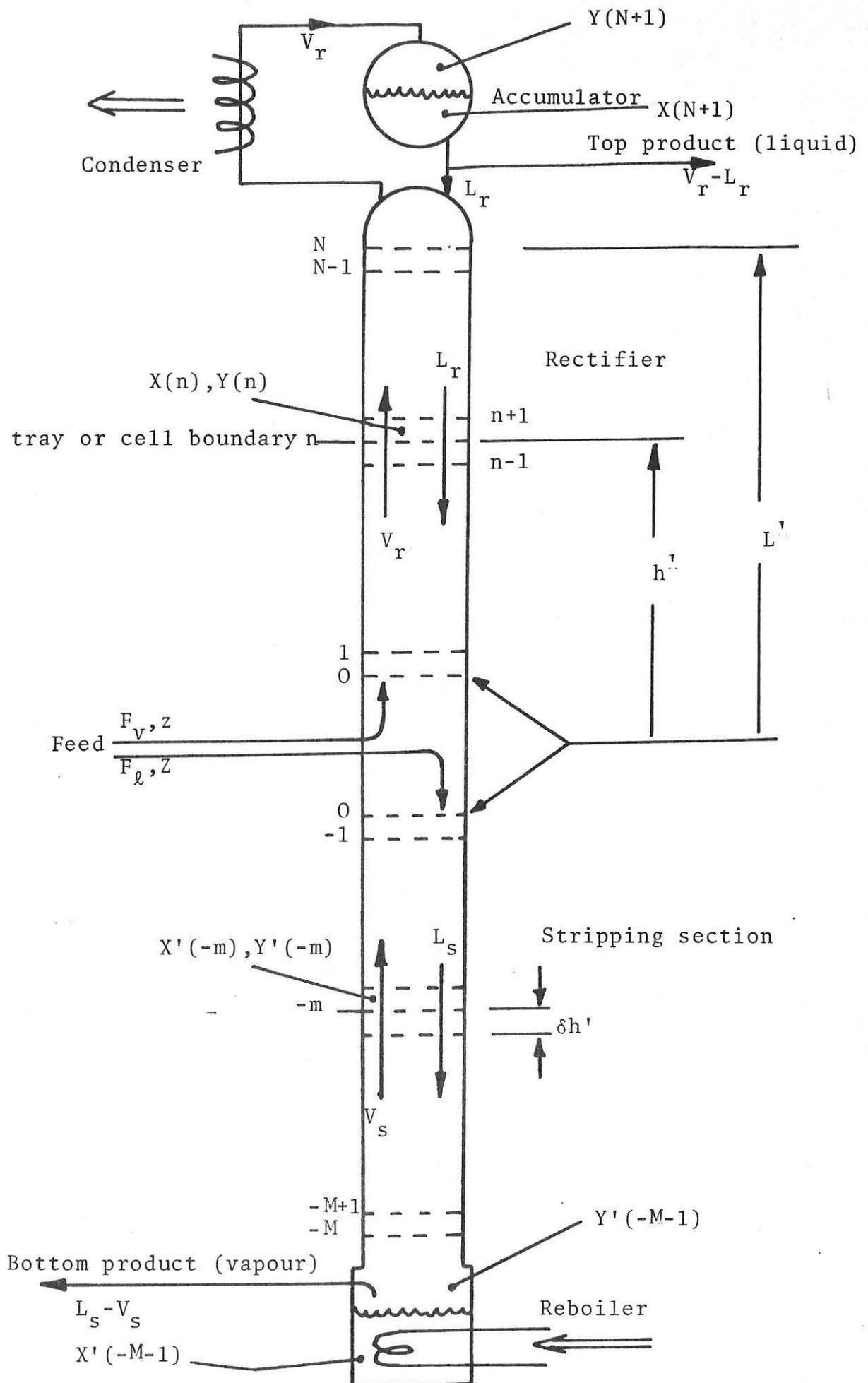   of liquid/liquid heat exchanger

Fig. 2.2   General arrangement of binary distillation column
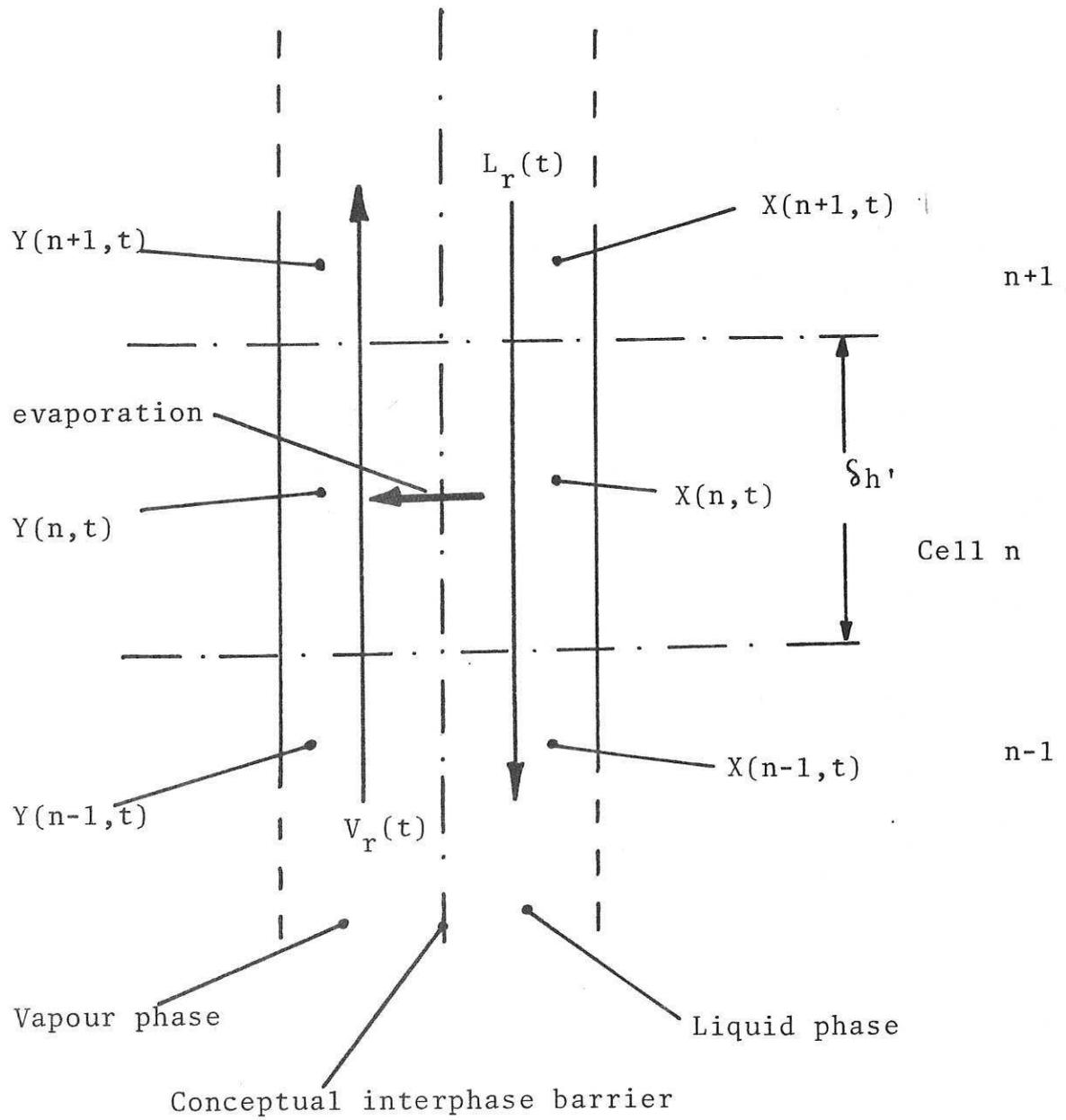
Fig. 2.3   Variables associated with n'th cell of
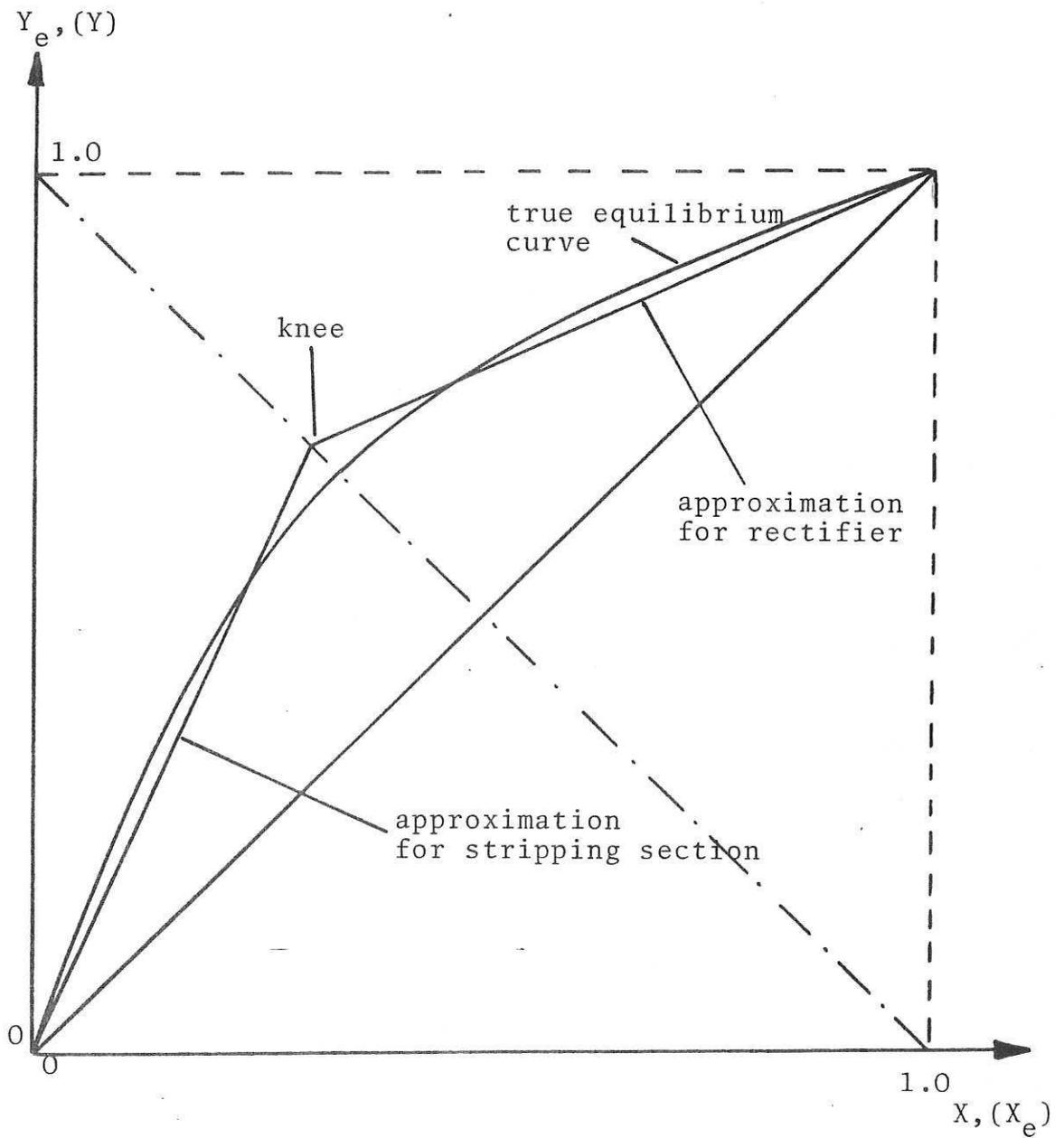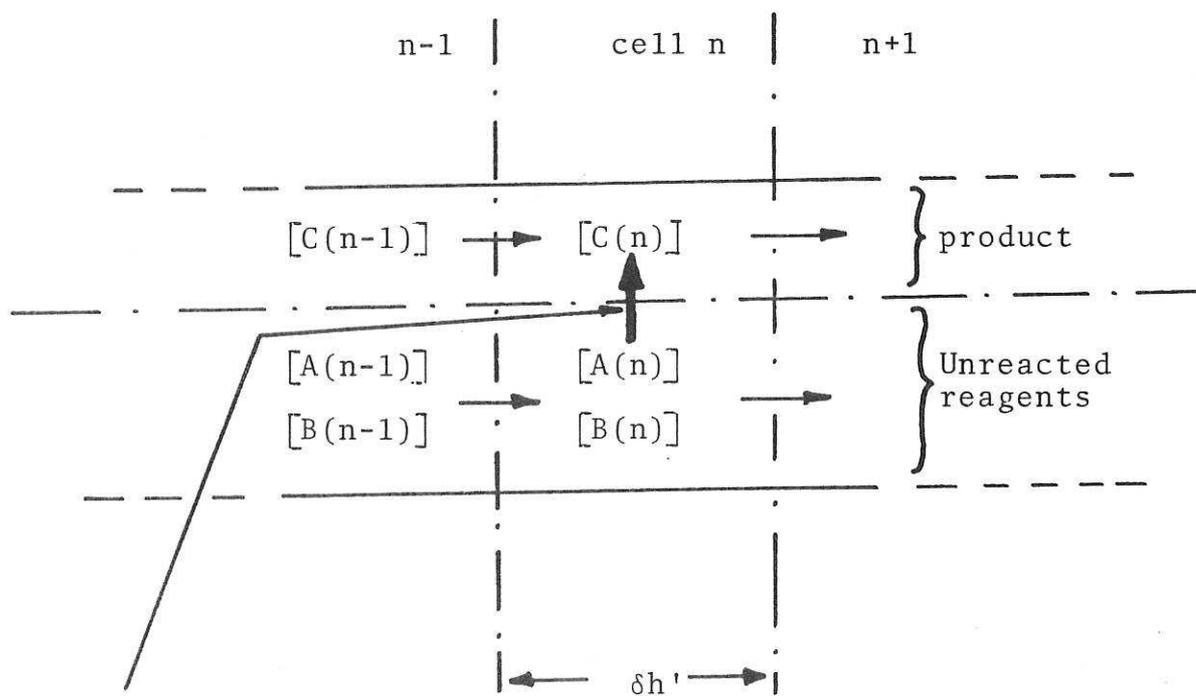   column rectifying section.

Fig. 2.4   Ideal equilibrium curve for binary mixture
            and its piecewise-linear approximation

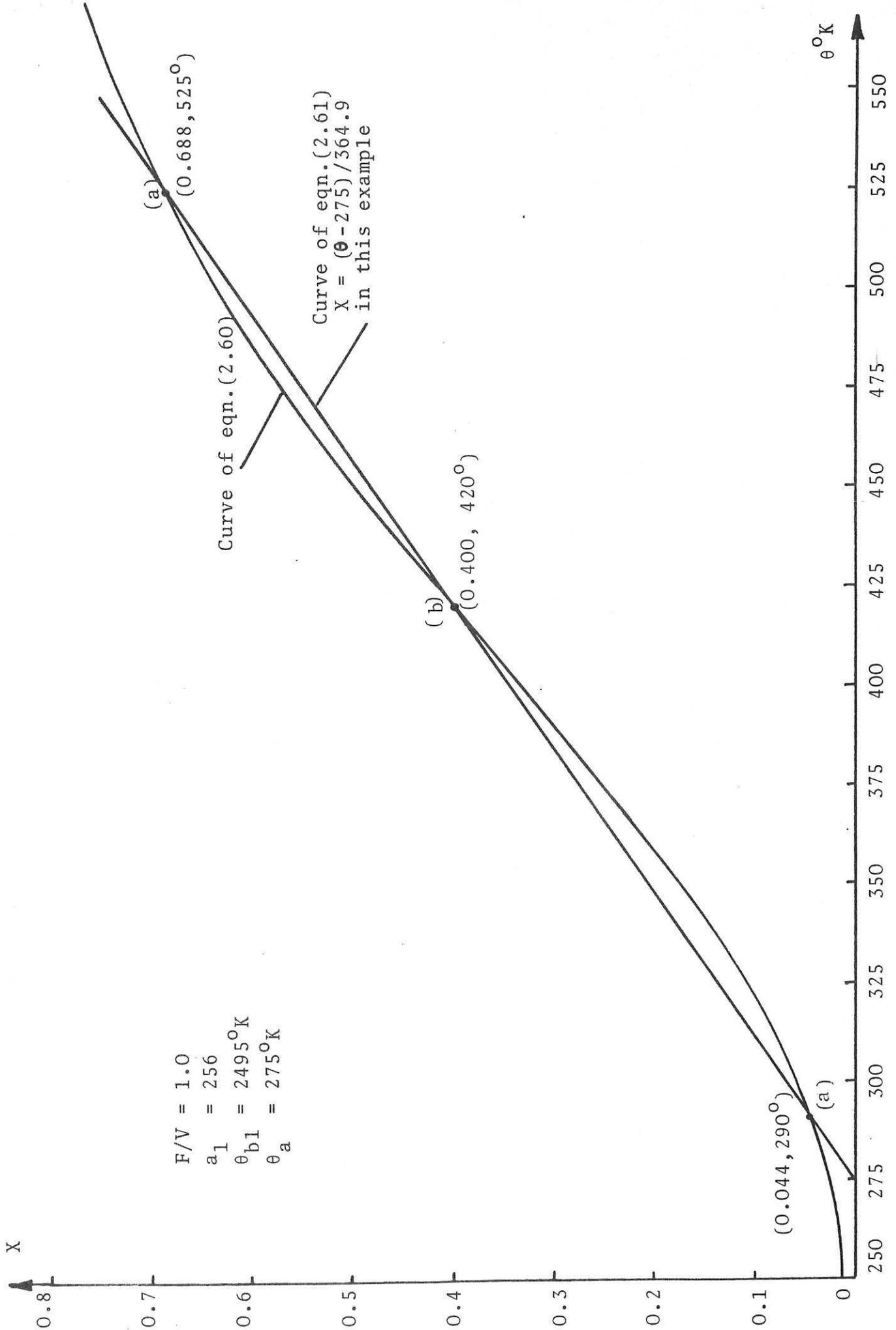Fig. 2.5   Conceptual model for tubular chemical reactor

Fig. 2.6   Showing possibility of triple solutions to steady-state reactor equations
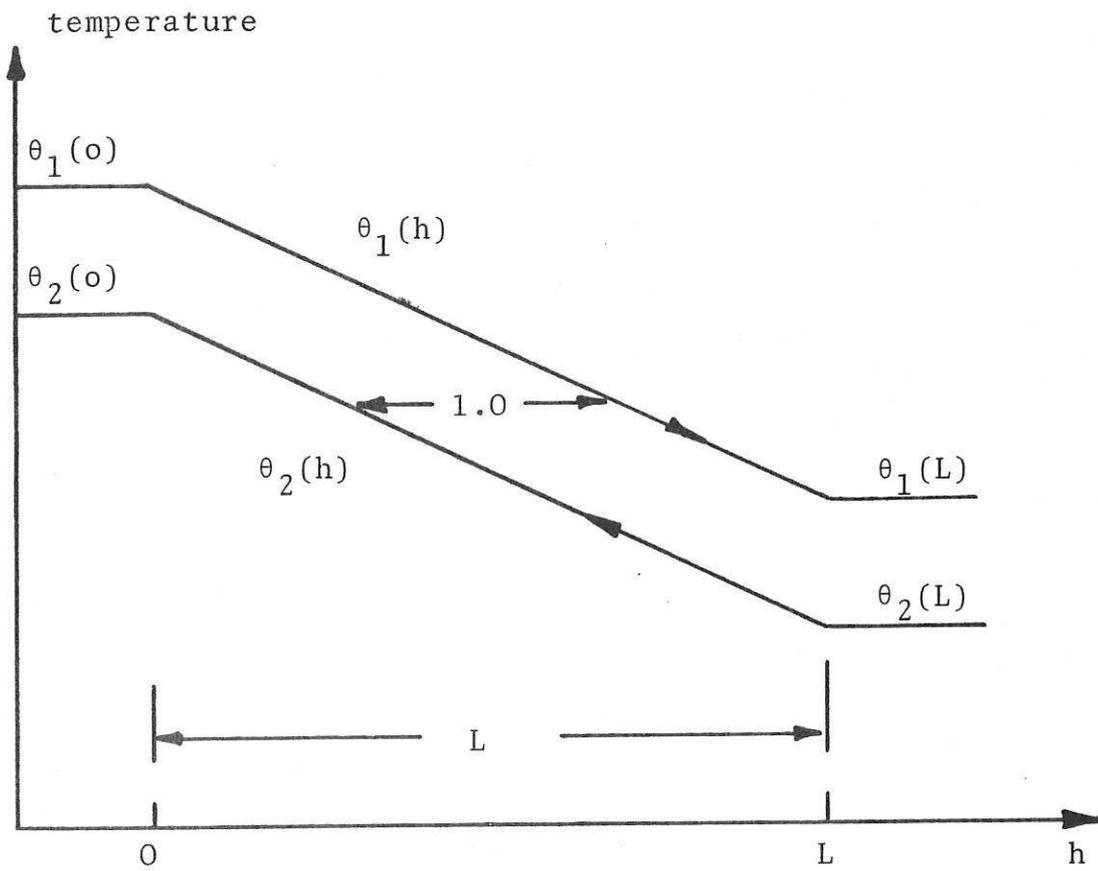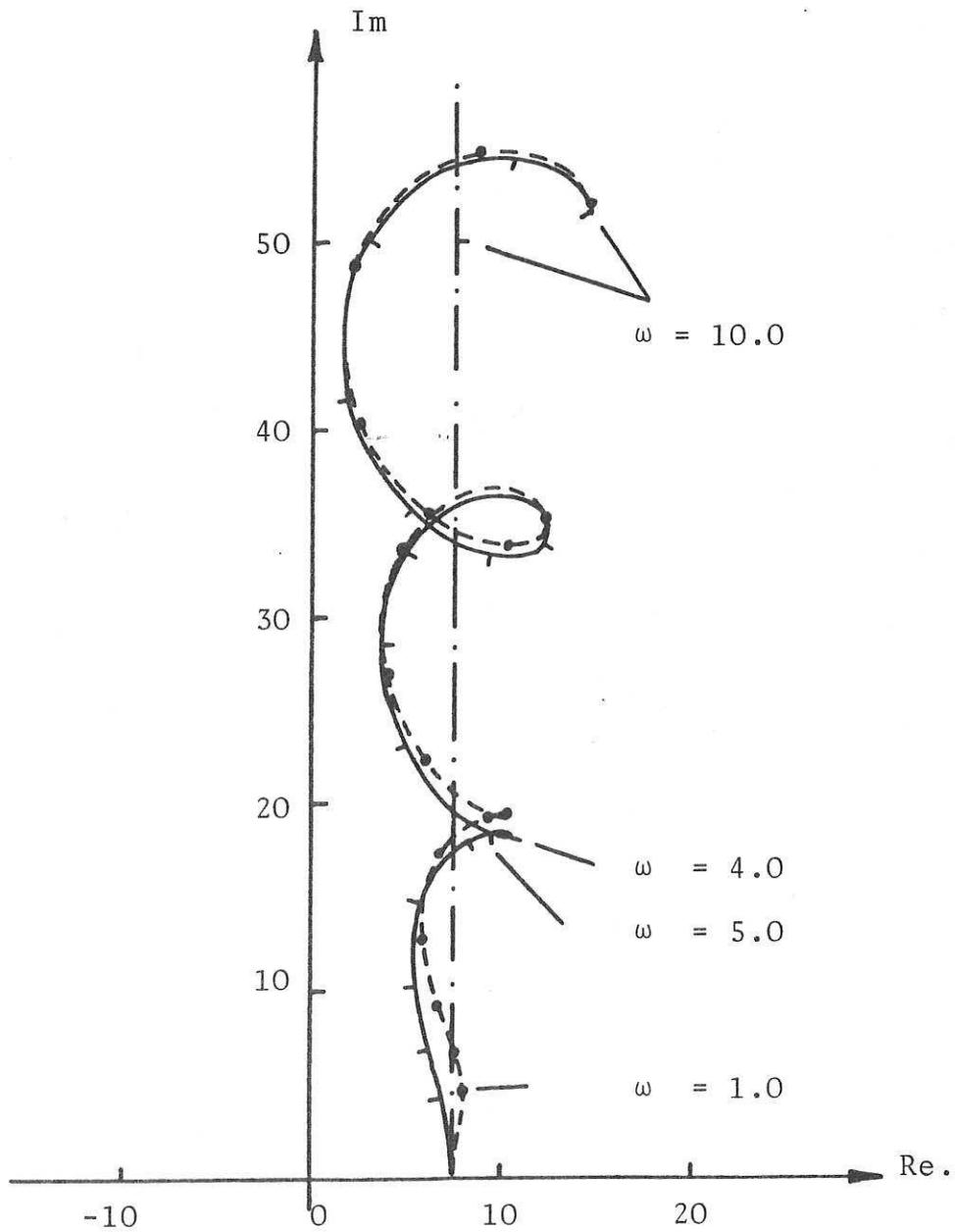
The figure shows a plot with X on the vertical axis (from 0 to 0.8) and $\theta °K$ on the horizontal axis (from 250 to 550).

Parameters shown:
$F/V = 1.0$
$a_1 = 256$
$\theta_{b1} = 2495°K$
$\theta_a = 275°K$

Curve of eqn.(2.60)

Curve of eqn.(2.61)
$X = (\theta - 275)/364.9$
in this example

Points marked:
(a) $(0.044, 290°)$
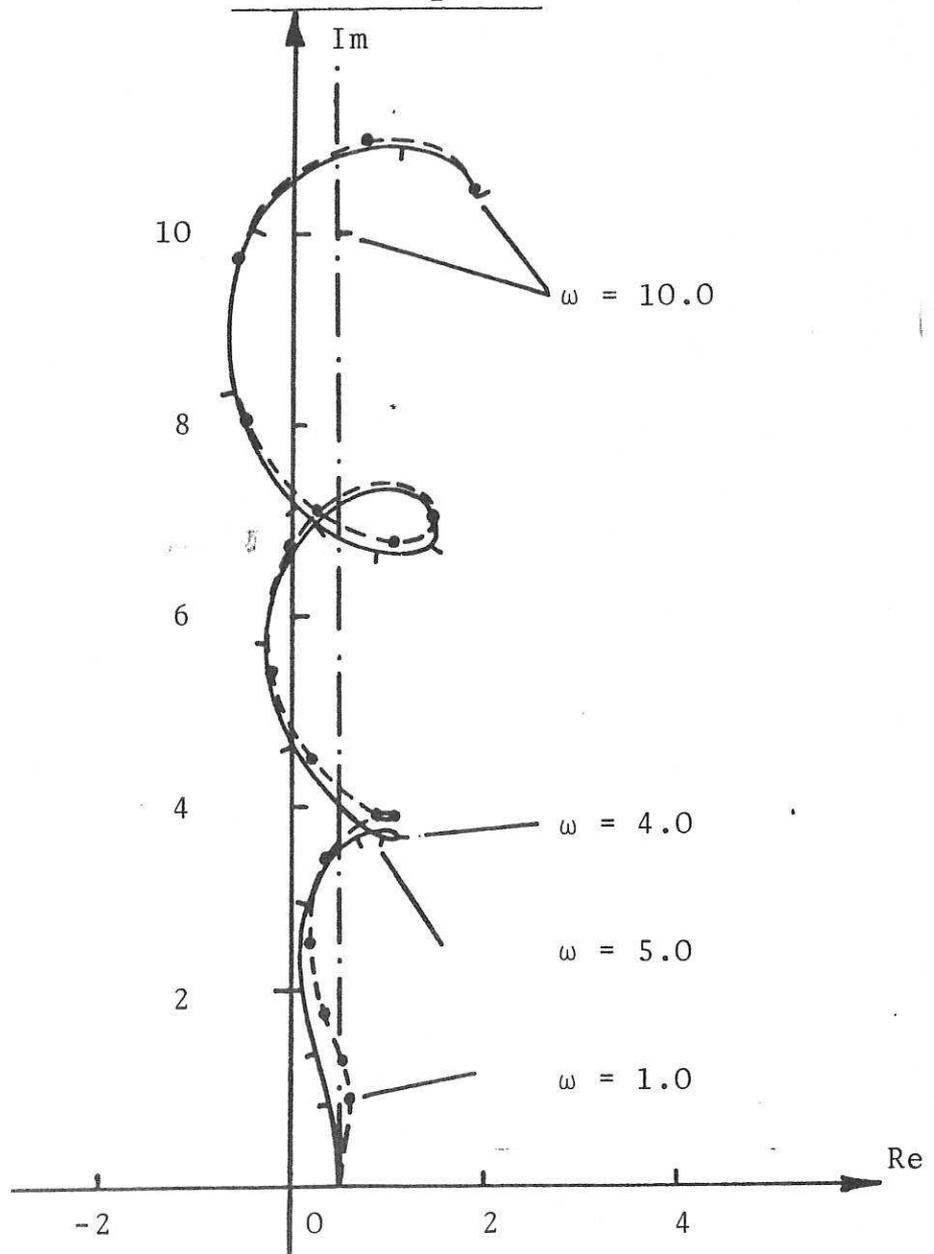(b) $(0.400, 420°)$
(a) $(0.688, 525°)$

Fig. 2.7   Steady state temperature profiles for
            symmetrical heat exchanger.

Fig. 2.8 Locus of $g_1^{-1}(j\omega)$

---
true system locus

- - - - - - lag/delay approximation

—.——.—— m.v. 1-st order lag approximation

ω - increment = 0.5 except where indicated otherwise

Fig. 2.9 Locus of $g_2^{-1}(j\omega)$

———————— true system locus

— — — — — lag/delay approximation

—·—·—·— m.v. 1-st order lag approximation

ω - increment = 0.5 except where indicated otherwise

Fig. 2.10. Steady-state composition profiles
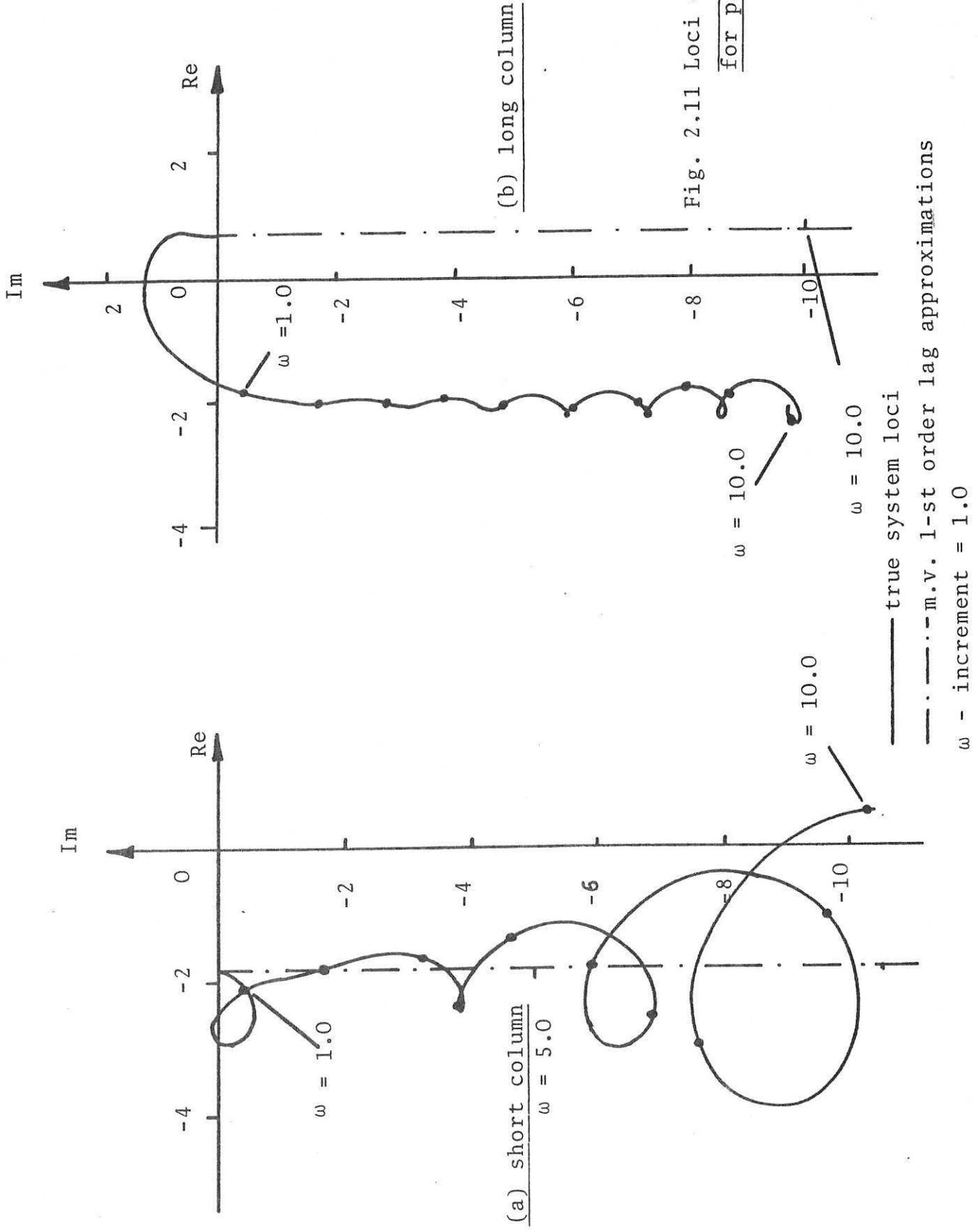
Re

Im

2

0

−2

−4

−6

−8

−10

ω =1.0

ω

ω = 10.0

(b) long column

Fig. 2.11 Loci of $g_1^{-1}(o,j\omega)$
for packed columns

—————— true system loci

—·—·— m.v. 1-st order lag approximations

ω − increment = 1.0

ω − increment = 1.0

Re

Im

0

−2

−4

−6

−8

−10

ω = 10.0

ω = 1.0

ω = 5.0

(a) short column